research report

Resistance of Arc Spot Welds – Update to Provisions

Committee on Specifications

for the Design of Cold-Formed

Steel Structural Members

American Iron and Steel Institute

DISCLAIMER

The material contained herein has been developed by researchers based on their research findings and is for general information only. The information in it should not be used without first securing competent advice with respect to its suitability for any given application. The publication of the information is not intended as a representation or warranty on the part of the American Iron and Steel Institute or of any other person named herein, that the information is suitable for any general or particular use or of freedom from infringement of any patent or patents. Anyone making use of the information assumes all liability arising from such use.

PREFACE

The American Iron and Steel Institute (AISI) Standards Council selected this project as one of four winning research proposals for its 2015 Small Project Fellowship Program. Project selections were based on several factors, including the potential for long-term impact on the industry; steel industry engagement and co-funding; and results for the AISI standards development committee, the student, and the academic institution.

The objective of this project was to evaluate the provisions for determining the strength of arc spot welds in light of recent research studies. It is anticipated that the results of this study will impact the provisions in future editions of AISI S100 and guide future research and development efforts.

RESISTANCE OF ARC SPOT WELDS – UPDATE TO PROVISIONS

By

B. PAIGE BLACKBURN, E.I.
1st LT, CIVIL ENGINEERING OFFICER, U.S. AIR FORCE
RESEARCH ASSOCIATE

THOMAS SPUTO, PH.D., P.E., S.E., SECB
ACADEMIC ADVISOR

CEVYN MEYER, P.E.
VULCRAFT DIVISION, NUCOR

FEBRUARY 2016
REVISED MAY 2018

ENGINEERING SCHOOL OF SUSTAINABLE INFRASTRUCTURE & ENVIRONMENT
UNIVERSITY OF FLORIDA
GAINESVILLE, FLORIDA

ABSTRACT

The provisions of the AISI S100-12 standard for strength of arc spot welds loaded in shear and tension have not been revised since the 1999 standard. Since then, four new research studies have created and tested arc spot welded connections, expanding the database of available tests. Therefore, a reconsideration of both the resistance equations and the resistance and safety factors using the enlarged data base was undertaken. This study performed a comprehensive analysis of the entire arc spot weld data base, where 450 specimens were categorized by their respective failure modes to assess current AISI S100-12 resistance equations. Performance of the existing equations was re-evaluated and compared with the performance of equations used in previous AISI S100 editions.

This study found that current equations and resistance and safety factors for sheet tearing failure modes are conservative and could be relaxed for shear as well as tension loading. New distinctions are proposed to improve the performance of side-lap connection resistance calculations. Also, removing the upper limit and adding a lower limit to the effective weld diameter calculation sharpened accuracy for calculated weld resistance of arc spot welds made through thicker sheet connections. Most AISI S100-12 equations were found to be adequate and can be made less conservative, however current provisions for weld failure under tensile load were found to substantially over predict weld strength. Adjustments to the tension weld resistance equation are recommended by this study to improve performance, however future research on tension weld failure of combined sheet connections would be beneficial.

TABLE OF CONTENTS

LIST OF FIGURES

LIST OF VARIABLES

β = Target reliability index, taken as 3.0, 3.5 or 4.0 based on AISI S100-12 specs

C_p = Correction factor (AISI S100-12 F1.1)

C_ϕ = Calibration coefficient (AISI S100-12 F1.1)

COV = Coefficient of variation

d' = Weld overlap onto top sheet on a side-lap connection, as used by LaBoube (1991)

d = Visual diameter of arc spot weld

d_a = Average diameter

d_e = Effective weld diameter at the plane of failure

E = Modulus of elasticity of sheet steel, taken as 29,500 ksi

F_m = Mean value of fabrication factor (AISI S100-12 F1.1)

F_u = Ultimate tensile strength of sheet steel

F_y = Yield tensile strength of sheet steel

F_{xx} = Ultimate tensile strength of weld metal

L = Length of top flange on a side-lap connection, as used by LaBoube (1991)

M_m = Mean value of material factor (AISI S100-12 F1.1)

n = Total number of samples included in the specific analysis

Ω = Omega, safety factor calculated for use in ASD

P_m = Mean value of professional factor (AISI S100-12 F1.1)

P_n = Calculated predicted resistance of arc spot weld connection

P_t = Ultimate load at failure during specimen testing

ϕ = Phi, resistance factor calculated separately for use in either LRFD or LSD

r = proposed reduction coefficient applied in resistance calculations

7

t = total combined thickness of sheets

V_F = Coefficient of variation of fabrication factor (AISI S100-12 F1.1)

V_M = Coefficient of variation of material factor (AISI S100-12 F1.1)

V_P = Coefficient of variation of test results (AISI S100-12 F1.1)

V_Q = Coefficient of variation of load effect (AISI S100-12 F1.1)

CHAPTER 1
INTRODUCTION

Corrugated sheet steel diaphragms are often used within lateral load resisting systems and as well as roof applications. These corrugated diaphragms are composed of thin rectangular cold formed steel sheets typically ranging from 22 to 16 gauge thickness, covering a range of 0.028 inches to 0.060 inches (0.72 mm to 1.52 mm) thick. Sheet diaphragms transfer load to the underlying steel frame through either arc spot welds or mechanical fasteners. Arc spot welds are popular as they can be created rapidly and cost effectively.

To transfer shear and tensile forces arc spot welds are placed around diaphragm edges and through its main section as pictured in Figure 1.1. Connecting adjacent diaphragms together results in one, two, and four sheet overlaps whose combined thicknesses must be penetrated by the arc spot weld. The current equations in AISI S100-12 for arc spot welds are predominately based on Pekoz and McGuire's 1979 report for shear strength equations and on LaBoube's 1991 report for tension strength equations. Since these reports were published additional authors explored thicker sheet welding and various multi sheet configurations typically found in practice to bolster the existing arc spot weld data base. This study takes a comprehensive look at the entire data base of new and old data to re-evaluate the existing arc spot weld strength equations in AISI S100-12.
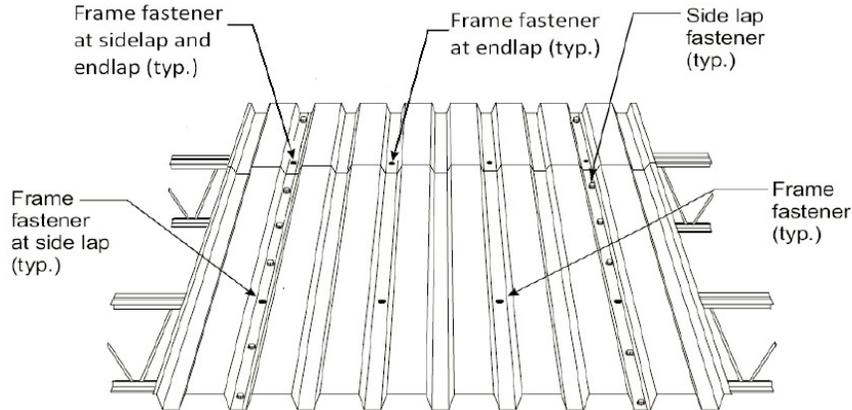
Figure 1.1: Typical arc spot locations (Guenfoud, 2010).

Creating an Arc Spot Weld

Arc spot welds are created by producing an electrode arc on the top sheet surface, forming a hole, heating up the base member (typically a hot rolled open-web steel joist) to ensure proper fusion and slowly moving the electrode in a circular motion filling the hole with weld metal until the hole is filled and proper fusion is achieved. Weld diameter is one major factor in the connection strength. Different weld diameter nomenclature includes: the visual diameter, d, measured at the surface of the top sheet; average diameter, d_a, defined as the average weld diameter from the bottom of the weld to the top sheet surface; and finally the effective weld diameter, d_e, the diameter of the weld at the plane of failure (see Figure 1.2). Calculation of effective and average weld diameters, d_e and d_a, is based on the visible diameter and total combined sheet thickness, t.
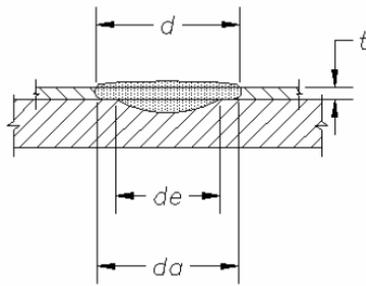
Figure 1.2: Arc spot weld diameters defined by AISI S100-12.

Failure modes

Arc spot welds fail in one of two general ways; either via sheet failure or via weld failure. This is true of both shear and tension loaded specimens. Shear failure through the weld, pictured in Figure 1.3, is typical when the ratio of weld diameter to total sheet thickness (d/t) is low. The result is a brittle failure mode where the weld metal reaches its ultimate load-carrying capacity before the sheet steel begins to deform and strain. In this case, the thicker combined sheets provide more shear resistance than a small weld can support.

Figure 1.3: Shear weld failure (Guenfoud, 2010).

Under shear loading, sheet failure occurs in either tearing or bearing behavior, both of which are associated with a larger diameter to thickness ratio (d/t). Sheet tearing, illustrated in Figure 1.4, begins on the tension side of the connection and propagates perpendicular to the direction of loading along the perimeter of the weld circumference as load is increased. As the

11

tearing propagates, the compression side of the connection distorts out of plane. The tearing and deformation results in a ductile failure mode compared to the weld shear failure mode. A sheet bearing failure is also ductile, but instead of tearing, the weld plows through the sheet material parallel to the shear load and sheet metal deforms and piles up in front of the weld path as pictured in Figure 1.5. In both sheet tearing and bearing failure modes, the weld strength is stronger than the shear resistance provided by the sheet(s).

Figure 1.4: Sheet tearing failure mode (Guenfoud, 2010).

Figure 1.5: Sheet bearing failure mode (Guenfoud, 2010).

Tension failure also occurs via the sheet or through the weld. Tension weld failure develops when the diameter to sheet thickness ratio (d/t) is very low, and proves to be a rarer occurrence compared to other failure modes within the data base. Weld failure takes place through the effective weld diameter and in a violent, brittle manner. Figure 1.6 illustrates tension

weld failure on a multi sheet connection where almost no sheet deformation can be noted. Tension sheet failure on the other hand exhibits significant sheet deformation as presented in Figure 1.7. As the sheet deforms under the tensile load, it creates concentrated stresses at the weld perimeter resulting in sheet tearing. Once sheet tearing initiates, the tear propagates about the weld perimeter in a circular fashion. Tension sheet failure is ductile in nature due to the substantial sheet deformation. This study reviews the AISI S100-12 equations associated with each of these failure modes.

Figure 1.6: Tension weld failure (Guenfoud, 2010).

Figure 1.7: Tension sheet failure (Guenfoud, 2010).

Objective

The arc spot weld strength equations in AISI S100-12 have not been examined with new data since 1999. This study re-evaluates the AISI arc spot weld strength equations with the entire

existing data base including hundreds of new specimens tested within the last seventeen years.

Resistance and safety factors for LRFD, ASD, and LSD were re-calculated for monostatic shear

and tension loading design equations. The equations themselves were also evaluated for accuracy

and applicability to various sheet configurations. A total of 1,193 arc spot weld specimens were

uncovered, making up the entire data base, while 450 of those were determined applicable to this

study.

Design Standards

AISI S100-12 design equations for sheet to base metal arc spot welds were reviewed. The

equations below are presented in the order that exists in the AISI specification and will be

referenced throughout this report. AISI S100-12 shear strength equations E2.2.2.1-1 through

E2.2.2.1-4 are presented below as Equations 1-1 through 1-4. Existing and recalibrated resistance

and safety factors for LRFD, ASD, and LSD for these equations are presented and compared in

the results section.

$$P_n = \frac{\pi d_e^2}{4} 0.75 F_{xx} \qquad \text{(Eq. 1-1)}$$

$$\text{For } d_a/t \leq 0.815 \ \sqrt{(E/F_u)} : P_n = 2.20 t d_a F_u \qquad \text{(Eq. 1-2)}$$

$$\text{For } 0.815 \ \sqrt{(E/F_u)} < d_a/t < 1.397\sqrt{(E/F_u)}: P_n = 0.280 \left[1 + 5.59 \frac{\sqrt{E/F_u}}{d_a/t} \right] t d_a F_u \qquad \text{(Eq. 1-3)}$$

$$\text{For } d_a/t \geq 1.397 \ \sqrt{(E/F_u)} : P_n = 1.40 t d_a F_u \qquad \text{(Eq. 1-4)}$$

$$\text{Where: } d_e = 0.7d - 1.5t \leq 0.55d \qquad \text{(Eq. 1-5)}$$

$$\text{Where: } d_a = d - t \qquad \text{(Eq. 1-6)}$$

Equation 1-1 calculates the shear strength of the weld area, predicting the load at which

the weld metal itself fractures. Equations 1-2, 1-3 and 1-4 all represent sheet resistance and are

bounded by the ratio size of average weld diameter, d_a, to total design sheet thickness, t. AISI

S100-12 tension strength equations E2.2.3-1 and E2.2.3-2 are presented respectively in Equations 1-7 and 1-8. Similar to the shear equations, Equation 1-7 calculates the tension capacity of the weld metal and Equation 1-8 predicts the tensile strength of the sheets.

$$P_n = \frac{\pi d_e{}^2}{4} F_{xx} \qquad\qquad\qquad\text{(Eq. 1-7)}$$

$$P_n = 0.8(F_u/F_y)^2 t d_a F_u \qquad\qquad\qquad\text{(Eq. 1-8)}$$

CHAPTER 2
LITERATURE REVIEW

Shear Tests

Pekoz and McGuire's 1979 report "Welding of Sheet Steel" summarized five reports co-authored by Pekoz between 1971 and 1978. A total of 342 shear loaded welded samples were created and tested at Cornell University over this time period, 126 of them being arc spot welded. All samples were tested with monotonically increasing shear load. Six sheet thicknesses were tested: 10 gauge (0.138 inches, 3.24 mm), 12 gauge (0.108 inches, 2.66 mm), 14 gauge (0.079 inches, 1.90 mm), 18 gauge (0.052 inches, 1.21 mm), 24 gauge (0.028 inches, 0.61 mm) and 28 gauge (0.019 inches, 0.38 mm). All sheets tested were created from ASTM A446 either Grade A (F_y = 33 ksi and F_u = 45 ksi) or Grade E (F_y = 80 ksi and F_u = 82 ksi) steel. Each sheet sample was welded to a hot rolled ASTM A36 steel base plate of 7/16 inch (11.10 mm) thickness. Both single and double sheet configurations were tested. The maximum thicknessses welded for single sheets were the 10 gauge samples at 0.138 inches (3.24 mm) thick, and 0.155 inches (3.94 mm) measured for two 14 gauge sheets (0.079 in, 1.90 mm) in a double sheet configuration. The single sheet configuration tested by Pekoz is depicted in Figure 2.1 below. All samples were welded with E6010 electrodes. Most samples were welded by a steel fabricator or in laboratory conditions, while 31 samples were welded in "field" conditions and consequently resulted in lesser quality welds.
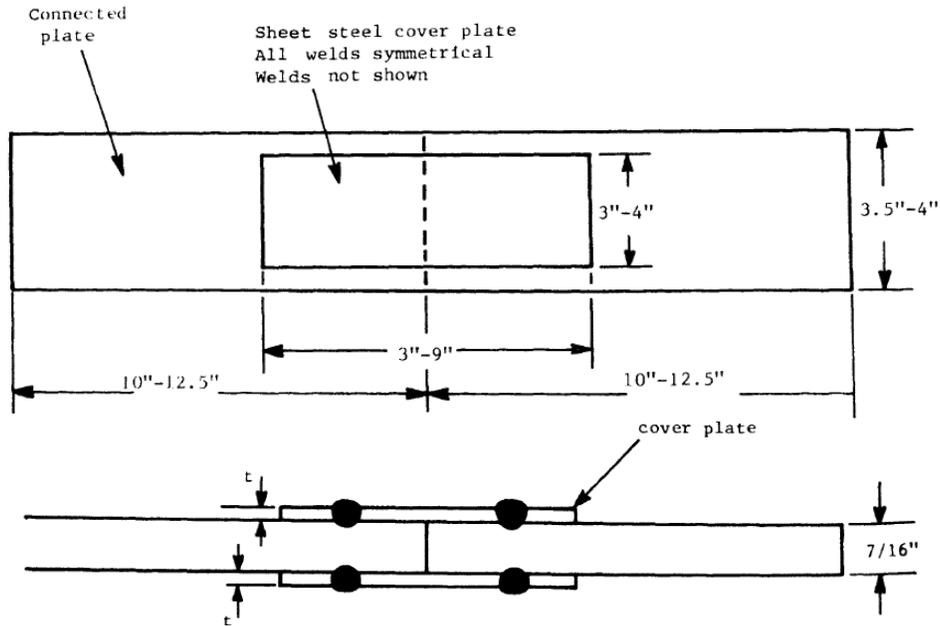
Figure 2.1: Single sheet configuration created by Pekoz (Pekoz, 1979).

Pekoz's work was initiated to codify sheet welding for the first time. His recorded failure modes and representative equations created the framework for what is currently codified in the AISI S100-12 standard for shear loaded sheet steel welds. Pekoz organized failure modes into three types: weld shear, sheet tearing, and sheet buckling. Most failures were preceded by out of plane sheet deformation. Weld shear failures were predicted with Equation 2-1, while all other failures were characterized by the ratio of weld diameter and sheet thickness (d_a/t) compared to ultimate strength of the sheet steel (F_u) and respectively predicted by either Equation 2-2 or 2-3. It should be noted that in the 1979 Pekoz report the equations are presented for two welds (as applicable to Pekoz's sample configuration), while the equations below are presented for a single weld.

$$P_n = \frac{\pi}{4} d_e{}^2 (0.75 F_{xx}) \qquad\qquad\qquad\text{(Eq. 2-1)}$$

For the range $140/\sqrt{F_u} \leq d_a/t \leq 240/\sqrt{F_u}$:

$$P_n = 0.280 \left[1 + \frac{960}{d_a\sqrt{F_u}} \right] t d_a F_u \qquad\qquad\qquad\text{(Eq. 2-2)}$$

17

For all other d_a/t ranges:

$$P_n = 1.40td_aF_u \qquad\qquad\qquad\qquad \text{(Eq. 2-3)}$$

Pekoz also developed Equation 2-4 to represent the effective weld diameter (d_e), defined as the diameter of the weld at the shear plane. He also created Equation 2-5 to represent the average weld diameter (d_a); both equations are still specified in AISI S100-12.

$$d_e = 0.7d - 1.5t \qquad\qquad\qquad\qquad \text{(Eq. 2-4)}$$

$$d_a = d - t \qquad\qquad\qquad\qquad\qquad \text{(Eq. 2-5)}$$

Fung's 1978 report "Strength of Arc-Spot Weld in Sheet Steel Construction" was the first of its kind completed for the Canadian Steel Industry Construction Council (CSICC), as the design community began to consider arc-spot welds structurally important. Fung split his focus into three different test series which included 127 shear specimens and 128 tension specimens. All samples were manually created with an E6010 electrode with a 5/32 inch (3.96 mm) diameter. Weld diameters were specified to 0.75 inches (19.05 mm) (with exception of test series three). Sheet steel material was ASTM A446, G-90, of either Grade A (F_y = 33 ksi) or Grade D (F_y = 50 ksi). Sheet thicknesses ranged from 0.030 to 0.060 inches (0.726 to 1.524 mm). Sheets were welded to plates composed of CSA G40.21 44W (F_y = 44 ksi) steel which had thicknesses that varied from 0.125 to 1.00 inches (3.18 to 25.4 mm).

Test series one included 96 samples that focused on developing a standardized weld technique and explored relationships between weld machine settings, weld technique, sheet thickness, plate thickness, and weld diameter. Fung concluded that the ratio of plate to sheet thickness should be equal to or greater than 2.5 in order to achieve proper fusion and that weld

settings should be adjusted to achieve an effective weld diameter of at least 0.45 inch (11.43 mm) for a 0.75 inches (19.05 mm) specified visible weld diameter.

Test series two explored weld capacities for shear loading and tension loading (applied separately). Figure 2.2 depicts Fung's shear configuration (note that the sheet on top, is drawn thicker at the weld for understanding but is thinner than the plate, on bottom). Plate thickness was 0.5 inches (12.7 mm) for all test series two samples and sheets varied from 0.031 to 0.059 inches (0.787 to 1.499 mm) thick. Unfortunately, Fung did not report the failure mode of each sample, he did write that all shear samples experienced out of plane deformation and a majority of samples exhibited sheet tearing in front of the weld. Fung used AWS D1.3-77 equations (Equations 2-6 through 2-9 below) to predict shear strength which he found to be slightly conservative.

Figure 2.2: Shear specimen created by Fung (Fung, 1978).

If $d/t < \frac{240}{\sqrt{F_y}}$: $P_n = 2.2td_aF_t$ (Eq. 2-6)

Where $F_t = 0.4F_u$ (Eq.2-7)

If $d/t \geq \frac{240}{\sqrt{F_y}}$: $P_n = 1.4td_aF_t$ (Eq. 2-8)

$P_n = \frac{\pi}{4}d_e^2(0.30F_{xx})$ (Eq. 2-9)

Test series three investigated several potential factors affecting weld strength which included: plate to sheet thickness ratios, strength of sheet material, weld size, surface coatings, initial gap between sheet and plate, different welders, and weld time. Specimens were prepared and tested in the same manner of test series two but varied the factors mentioned above. Fung found that heavily galvanized surfaces and air gaps lowered weld capacity, while strength of sheet material and welds larger than 0.75 inches (19.05 mm) had little effect on the weld

capacity. Arc time was directly related to weld size and thereby load capacity in the case of welds smaller than 0.75 inches (19.05 mm). Therefore, shorter weld durations yielded smaller welds and lower strengths. Fung reported that a standardized weld technique proved to be the most important factor on weld capacity.

Peuler's 2002 report "Inelastic Response of Arc-Spot Welded Deck-to-Frame Connections for Steel Roof Deck Diaphragms" explored how to improve arc spot weld strength in a seismic environment. His research included 235 monotonic, cyclic and seismic shear loading tests. Within these loading types Peuler researched the effects of weld washers versus no reinforcement as well as different electrode types to produce the best arc spot weld. His sheets were composed of ASTM A635 steel and 16 gauge (0.060 inches, 1.52 mm), 18 gauge (0.052 inches, 1.21 mm), 20 gauge (0.036 inches, 0.91 mm) and 22 gauge (0.030 inches, 0.76 mm), three different plate sizes were used ranging from 1/8 to 1/2 inches (3.18 mm to 12.7 mm) thick, and three different weld washer shapes were tested. Figure 2.3 illustrates the shear test assembly employed by Peuler.
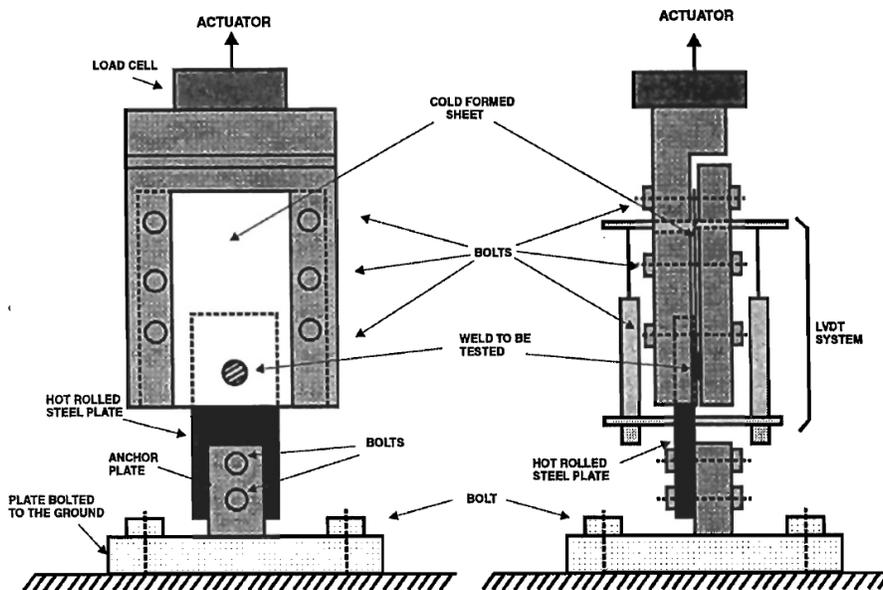
Figure 2.3: Shear test assembly used by Peuler (Peuler, 2002).

Although focused on seismic loading, Peuler's work included 49 monotonically loaded shear single sheet samples that were created without weld washers. These samples were created with varied plate thicknesses and weld electrodes and are included in this analysis. Peuler had 4% of his samples fail through the weld, all of which included a weld washer. He measured the effective weld diameter of the failed samples and noted that Equation 1-5 was generally conservative. He also noted that E6011 electrodes exhibited the best penetrating power over E6010, E6022 and E7018 electrodes.

Easterling and Snow investigated reduced welding time and multi-sheet welding in their shear tests reported in the 2008, "Strength of Arc Spot Welds Made in Single and Multiple Steel Sheets". Samples were welded with 1/8 inch (3.18 mm) diameter E6010 electrodes at full weld time, 2/3 weld time, and 1/3 weld time. Single, double, and four sheet thicknesses of ASTM A653 Grade 33 steel 16 to 22 gauge were welded and tested; making up the 138 specimens tested. Test results were then used to evaluate the 2001 AISI shear specifications for arc spot welds. Easterling's specimen assembly tested is illustrated in Figure 2.4.
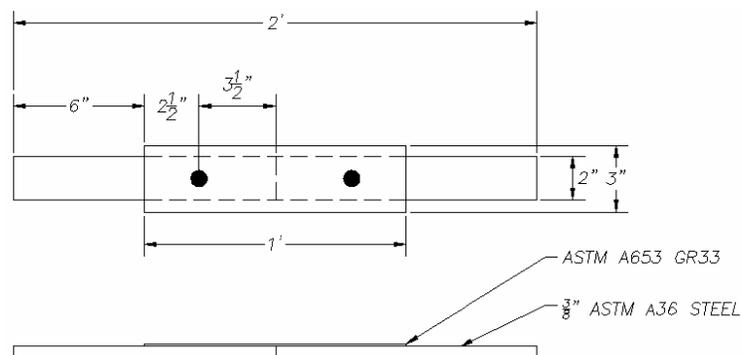
Figure 2.4: Specimen dimensions used by Easterling and Snow (Easterling and Snow, 2008).

Easterling and Snow found that the 2001 AISI shear strength equations were adequate when estimating the strength of the 2/3 and 1/3 weld time specimens by using the visual weld diameter. The test failure loads were on average 30% higher than the strength predicted by AISI

21

S100-12 shear equations, but they found the accuracy of these equations diminished for thicker sheet samples and shorter weld durations. Easterling and Snow recommended that sheets with combined thicknesses larger than 0.15 inches (3.81 mm) should not be used in arc spot welded connections. Note this was the conclusion when using E6010 electrodes.

Expanding from the scope of existing data, Guenfoud's 2010 report, "Experimental Program on the Shear Capacity and Tension Capacity of Arc-Spot Weld Connections for Multi-Overlap Roof Deck Panels" investigated shear and tension capacities for arc-spot welds through one to four sheet thicknesses. Welding through four sheets commonly occurs at the overlapping corners of four different deck panels as illustrated in Figure 2.5. Guenfoud performed monotonically loaded tension and shear tests as well as cyclic shear tests on a total of 179 specimens. Only the monotonic tests will be reviewed here.
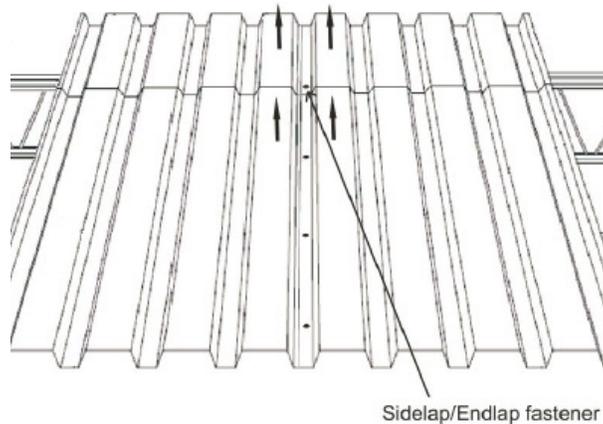
Figure 2.5: Arc-spot weld through four sheets as found in panel construction (Guendfoud, 2010).

Guenfoud paid particular attention to weld quality. E6011 electrodes with a 1/8 inch (3.18mm) diameter rod was chosen based on its ability to penetrate through thicker sheets as noted by Peuler's 2002 report. All of Guenfoud's samples were created by an experienced certified welder in collaboration with a weld engineer. Welds were circular with a visible diameter of 16 to 19 mm (0.63 to 0.75 inches). To maximize penetration and minimize porosity

Guenfoud found that an AC current of 195 amps worked best for 16 and 18 gauge sheets while 160 amps was best for 20 and 22 gauge sheets.

The sheet material was ASTM A653 Grade 33 steel (F_y = 33 ksi, F_u = 45 ksi) for all 76 monotonically loaded shear samples. Sheet thicknesses were 16, 18, 20, and 22 gauge. Sheets were welded onto a Grade 350W CSA G40.21 hot rolled plate of either 6.4 or 3.2 mm (0.252 or 0.126 inch) thickness. Three different sheet configurations were tested in shear. A two sheet side-lap configuration, in which the shear plane was located between the sheets (design thickness equals one sheet). A four sheet configuration as shown in Figure 2.5 featured the shear plane in the middle of the four sheets (design thickness equals two sheets). The third configuration mimicked a perimeter end lap connection between two sheets where the shear plane was located between the hot rolled plate and the two sheets (design thickness equals two sheets). Figure 2.6 pictures the shear test assembly used by Guenfoud and Figure 2.7 presents the perimeter sheet configuration.
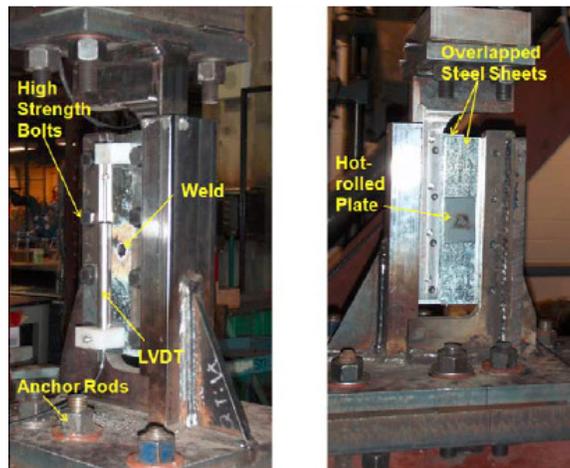
Figure 2.6: Shear test assembly used by Guenfoud (Guenfoud, 2010).
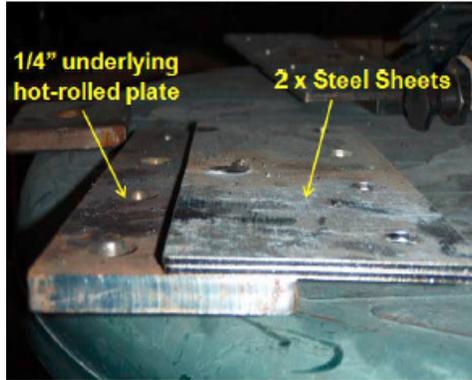
Figure 2.7: Perimeter shear configuration (Guenfoud, 2010).

Guenfoud recorded three different failure modes; shear failure through the weld, sheet tearing failure, and sheet bearing failure. For specimens that failed through the weld, Guenfoud was able to measure the effective weld diameter, d_e, with a vernier caliper. Guenfoud found that the current d_e equation (Equation 1-5) was conservative for welding through multiple sheet layers, particularly for connections with larger ratios of design thicknesses to weld diameter. Based on Guenfoud's analysis as depicted in Figure 2.8, he proposed Equation 2-10 as a modification to Equation 1-5.
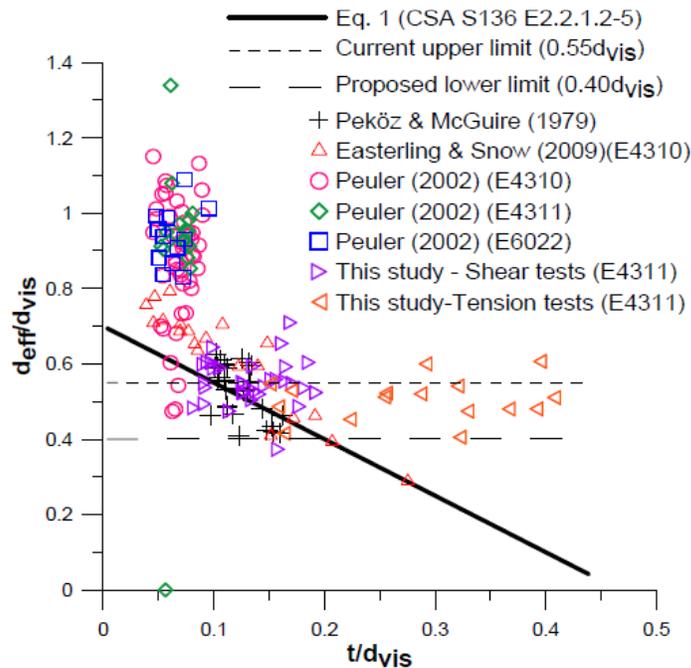
Figure 2.8: Shear weld failure samples from existing data base (Guendfoud, 2010).

24

$$d_e = 0.7d - 1.5t, \text{with } 0.4d \leq d_e \leq 0.55d \qquad\qquad \text{(Eq. 2-10)}$$

All specimens with one sheet above the shear plane failed in either sheet tearing or bearing failure modes (the thinner design thickness, t, specimens). All 16 and 18 gauge four sheet specimens and perimeter two sheet specimens failed through the weld, a total of 33 samples, making Guenfoud the largest contributor to the shear weld failure data base. The two sheet design thickness and the thickest of the sheets tested appeared to increase sheet resistance and force failure through the weld area. Alternatively, the 20 and 22 gauge specimens with four sheets resulted in various failure modes, but predominately sheet bearing failure.

Guenfoud's sheet failure specimens mostly fell into the category of AISI S100-12 equation E2.2.2.1-2 (Equation 1-2 above). He found Equation 2-11 to be the best fit for this category, the only change being a coefficient of 2.40 rather than 2.20. With this equation, Guenfoud recorded a measured to predicted ratio of 1.32, a coefficient of variation (COV) of 0.14 and a LSD resistance factor, ϕ, equal to 0.60.

$$\text{For } {}^{d_a}/_t < 0.815\sqrt{E/_{F_y}} : \quad P_n = 2.40td_aF_u \qquad\qquad \text{(Eq. 2-11)}$$

Tension Tests

Tension tests, 128 total, were conducted in Fung's 1978 report in addition to shear in all three test series. All parameters were the same between shear and tension tests, with the addition of the tension test setup pictured in Figure 2.9. Tension loading deformed the channel section of the sheet away from the weld which created non-uniform and concentrated stresses along the weld perimeter closest to the channel walls. Fung described this failure mode as a peeling effect of the sheet as it tore around the weld perimeter.

Fung's conclusion provided design weld shear and tension capacities for sheet thickness and grade in a tabular form based on test results, but he did not produce prediction equations beyond AWS D1.3-77. At the time, AWS did not specify tensile capacity equations for arc-spot welds, but Fung found that the ratio of shear strength to tension strength was fairly constant for different sheet thicknesses with a ratio ranging from 2.5-2.8 for all samples.
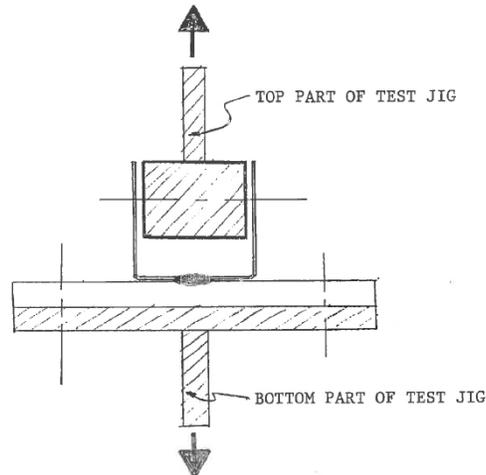
Figure 2.9: Tension specimen created by Fung (Fung, 1978).

In 1988, Albrecht's report "Developments and Future Needs in Welding Cold-Formed Steel" focused on analyzing Fung's tension data in order to develop a design equation for tensile strength of arc-spot welds. Albrecht proposed Equation 2-12 below for nominal tensile strength.

$$P_n = 0.9td_aF_u \qquad\qquad\qquad\qquad\text{(Eq. 2-12)}$$

This equation was further refined by Yu at the University of Missouri-Rolla in 1989. Yu modified Equation 2-12 to achieve a factor of safety equal to 2.5 which resulted in Equation 2-13. Following Yu's work, the American Iron and Steel Institute (AISI) adopted Equation 2-14 in a 1989 addendum to the 1986 Specification for the Design of Cold-Formed Steel Structural Members (LaBoube and Yu, 1991).

$$P_n = 0.66td_aF_u \qquad\qquad\qquad\qquad\text{(Eq. 2-13)}$$

$$P_n = 0.70td_aF_u \qquad\qquad\qquad\qquad\qquad\qquad\text{(Eq. 2-14)}$$

LaBoube and Yu's 1991 report "Tensile Strength of Welded Connections" published for the American Iron and Steel Institute expanded Fung's tensile data with 260 specimens composed of several different sheet configurations under tensile loading. These configurations are those commonly found in deck connection geometries that include single sheet interior welds, double sheet interior welds, side-lap welds, eccentrically loaded single sheet perimeter welds as well as full-panel tests. The test assembly for the concentrically loaded samples is pictured in Figure 2.10 demonstrating a single sheet configuration while double sheet interior weld and side-lap weld configurations are sketched in Figure 2.11. Eccentrically loaded samples were tested similar to Figure 2.10 with the exception that only one side of the channel was bolted into the test apparatus.
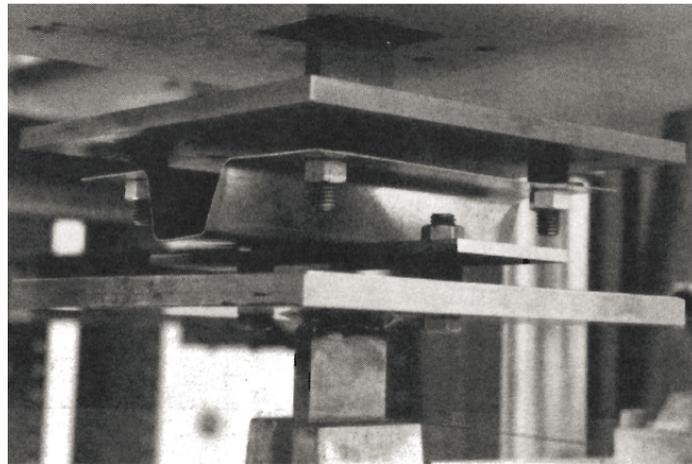
Figure 2.10: Single sheet configuration in tension test assembly (LaBoube and Yu, 1991).
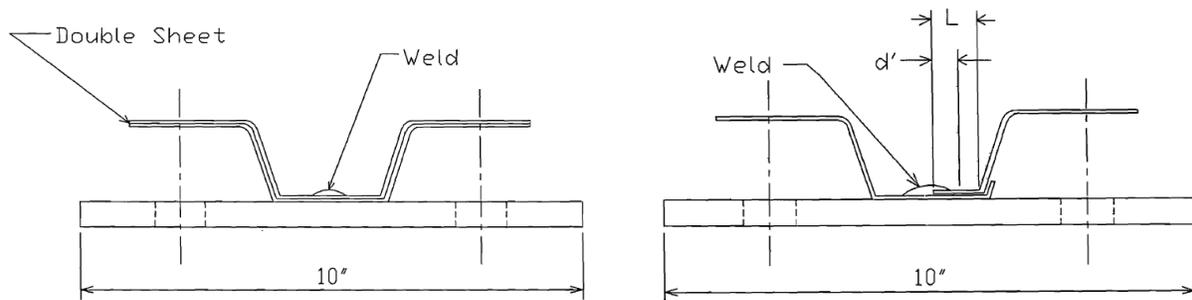
Figure 2.11: Double sheet interior weld and side-lap weld configurations (LaBoube and Yu, 1991).

In addition to these sheet configurations both stick and automatic welding procedures were investigated. For both processes an E70 electrode was used to create all samples. Sheet materials tested were ASTM A446 of either Grade C (F_u = 50 ksi) or Grade E (F_u = 82 ksi). The majority of samples were created with sheets 0.029 inches (0.737 mm) thick and a handful of specimens with 0.065 inches (1.651 mm) sheet thickness. Traditionally, weld washers were only used on sheets thinner than 0.028 inches (0.711 mm) at the time of LaBoube's report, but he created specimens for eccentric loading that included either round, rectangular, or no weld washers to explore their effect on sheet peeling caused by eccentric loading. Ten single sheet interior welds were also tested with weld washers.

LaBoube found that both stick and automatic weld processes produced quality welds of nearly equal strength, with the exception that automatic welding did not work well when using weld washers. Round and rectangular weld washers were found to equally improve the strength of eccentrically loaded specimens by reducing sheet peeling. The interior welds with weld washers forced the failure through the weld due to the added reinforcement to the sheet.

During testing, LaBoube observed specimens made of ASTM A446 grade C steel distorted more prior to failure than ASTM A446 grade E steel specimens due to increased

28

ductility. ASTM A446 grade C coupon tests performed by LaBoube resulted in 15% elongation while grade E resulted in 3% elongation. LaBoube related reduced ductility to higher strength steels and reflected this relationship in a new equation to predict tensile strength of arc-spot welds based on the ratio of ultimate stress to modulus of elasticity for sheet steel (Equation 2-15 and Equation 2-16 below). These equations were able to estimate the strength of single and double sheet configurations from both Fung's and LaBoube's data with a target reliability index (β) of 3.5.

$$\text{If } \frac{F_u}{E} < 0.00187: \; P_n = \left[6.59 - 3150 \left(\frac{F_u}{E}\right)\right] td_a F_u \leq 1.46 td_a F_u \qquad \text{(Eq. 2-15)}$$

$$\text{If } \frac{F_u}{E} \geq 0.00187: \; P_n = 0.70 td_a F_u \qquad \text{(Eq. 2-16)}$$

For side-lap configurations (shown on the left side of Figure 2.11) LaBoube tested samples with varied amount of weld overlap onto the top sheet bottom flange with length "L". He found that the amount of weld coverage was extremely influential on the strength of the connection. Even samples that had full weld coverage were not able to achieve strengths determined by Equations 2-15 and 2-16. It appeared that the unstiffened top flange transferred uneven loading to the connection and all failure modes resulted in tearing of the top flange away from the weld. LaBoube recommended reducing side-lap weld capacities by 30% from that calculated in Equations 2-15 and 2-16. Similarly for eccentrically loaded specimens the author recommended a reduction of 50% or to reinforce these welds with a weld washer to achieve the full predicted strength capacity. While Equations 2-15 and 2-16 predict strength of sheet tearing behavior, a few samples failed through the effective weld area. LaBoube proposed Equation 2-17 to account for this tension failure through the weld (similar to Pekoz's Equation 2-1 for weld failure in shear).

$$P_n = \frac{\pi}{4}d_e{}^2(F_{xx}) \hspace{4cm} \text{(Eq. 2-17)}$$

Guenfoud's 2010 report also included 72 tension loaded specimens in addition to monotonic and cyclic shear loading. All material properties and weld techniques are similar to that covered in the shear tests with the addition of Guenfoud's tension test assembly pictured in Figure 2.12. Tension tests included one, two (side-lap), and four (double side-lap) sheet configurations (see Figure 2.13). All one and two layer specimens failed by tearing through the sheet about the weld perimeter as well as most four layer specimens of 18, 20, and 22 gauge sheets. Alternatively, all four layer 16 gauge and some four layer 18 and 20 gauge samples failed through the weld area.
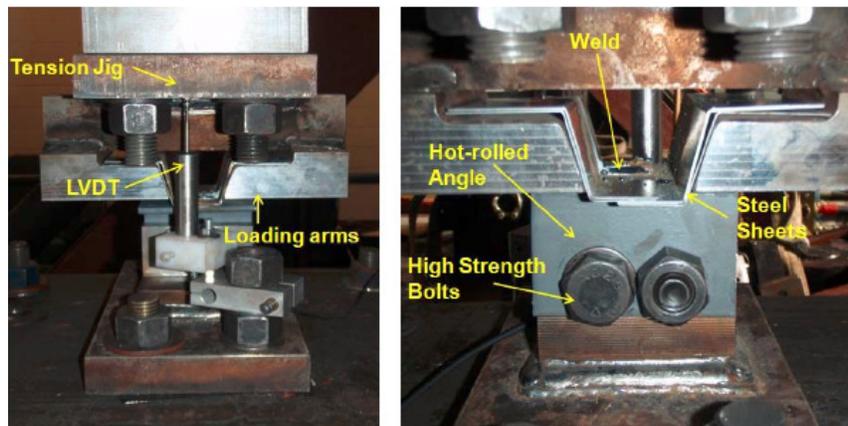
Figure 2.12: Tension test assembly used by Guenfoud (Guenfoud, 2010).
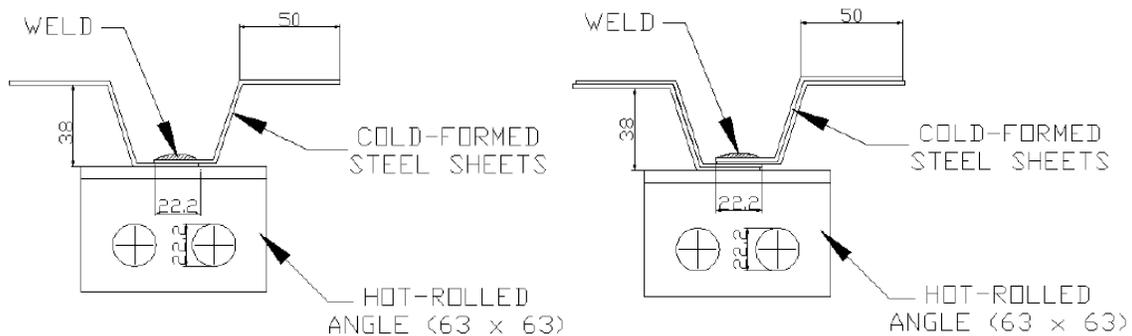
Figure 2.13: Two sheet lap (left) and four sheet side-lap (right) configurations (Guenfoud, 2010).

Failure appeared to occur at the mid-thickness of each two layer sample. Therefore, Guenfoud noted that the design thickness should be taken as one sheet, not two. Guenfoud

30

recommended no reduction for side-laps when using an appropriate length of an unstiffened flange. Appropriate length was defined as equal to or greater than the diameter of the weld (unlike LaBoube's side-lap specimens which featured partial coverage of the top sheet by the weld). With no reduction, Guenfoud was able to achieve a measured to predicted strength ratio of 1.17 and a COV of 0.28 based on AISI S100-12 equation E2.2.3-2 (Equation 1-8).

For Guenfound's 16 tension weld failures, 7 of which had a 3.2 mm (0.126 inch) base plate versus a 6.4 mm (0.252 inch) base plate, Guenfoud found that the thinner bottom plate would bend and create concentrated stresses on the weld and would result in peeling. Including data from both base plate thicknesses he recommended Equation 2-18, featuring a 50% reduction to account for peeling action. Using the measured effective weld diameter he achieved a measured-to-predicted strength ratio of 1.0 and COV of 0.27.

$$P_n = 0.5(\frac{\pi}{4}d_e{}^2F_{xx}) \hspace{4cm} \text{(Eq. 2-18)}$$

This study pulls data from all authors previously mentioned. Each set of data had to be treated separately, case by case, in order to compare all data together in one group. All assumptions and decisions that occurred during the data analysis in this study are noted in the following sections. The authors summarized above and others have performed arc spot weld testing beyond monotonic shear and tensile loading assessed in this study. Guendfoud included cyclic shear testing, LaBoube explored full diaphragm shear testing as well as combined shear and tension loading and Peuler tested specimens under cyclic and seismic shear loading. This report will focus solely on monotonic loading of individual welds and their existing design equations in AISI S100-12.

CHAPTER 3

ANALYSIS APPROACH

This study performed a comprehensive analysis on arc spot weld data from 1973 through 2010. AISI S100-12 arc spot weld strength equations, presented here as Equations 1-1 through 1-8, and their current resistance and safety factors were each evaluated using all applicable data. Note that only laboratory measured values such as F_u, F_y, d, and t, rather than their specified or nominal values, were implemented in the study to maintain accuracy. There is a challenge in combining data derived by multiple researchers who tested various configurations within their research. Some assumptions and exclusions were necessary as the data was combined. The analysis approach for each equation evaluated is systematically explained in the following sections below.

One decision that affected each analysis was how to handle Fung's data from 1978. Although he tested over 250 shear and tension samples, some pertinent data was not reported. Fung performed coupon tests but did not include the ultimate strength, F_u. An excerpt from his 1978 report is included in Figure 3.1, were F_y is included but not F_u. Albrecht's report in 1988 analyzed Fung's tension data, and included F_u values for Fung's sheet material properties. It appears Albrecht presented Fung's original F_y value as F_u in the appendix of his 1988 report. The authors here were unable to determine how Albrecht determined Fung's F_u values. Due to lack of information, Fung's data was excluded from this study for both shear and tension sheet failure analyses. Analysis of weld strength Equations 1-1 and 1-7 included Fung's data as they only require weld strength, F_{xx}, and not F_u. A comprehensive list of data included in this study in listed in Appendix A and is organized by the applicable AISI design equation.

TABLE 1

PHYSICAL AND WELDING DATA OF SPECIMEN FOR TEST SERIES II

Page 1 of 2   SHEAR TEST

SPECIMEN NO.	SHEET STEEL (ASTM A446 G-90)			PLATE STEEL		WELD DIAMETER (in)		WELDING DATA		
	THICK t (in)	GRADE	ACTUAL Fy (ksi)	THICK. T (in)	MATERIAL SPEC.	SPECIFIED	MEASURED	TIME (sec)	WELDER NO.	MELTING RATE (in/min)
2AS-101 -102 -103	0.031 " "	A " "	53.0 " "	0.5 " "	G40.21 44W " "	0.75 " "	.75 .75 .88	7.0 7.0 8.0	1 " "	13.1 " "

Figure 3.1: Sample of Fung's material properties table (Fung, 1978).

Shear: Weld Failure

Shear weld strength of arc spot welded connections is governed by Equation 1-1 (AISI S100-12 E2.2.2.1-1). In this failure mode the connected sheets remain intact, but the weld metal has been sheared through. The authors who experienced this type of shear failure (without the use of weld washers) included 33 samples from Guenfoud, 24 from Pekoz, 19 from Snow and Easterling, and 11 from Fung for a total of 87 samples. Fung's data was included because Equation 1-1 is based on ultimate weld strength (F_{xx}) which Fung reported, unlike ultimate sheet strength (F_u) which could not be confirmed in this study as previously mentioned. Only full time welds from Snow and Easterling's report were included in this study.

Pekoz's 1979 report has an additional 13 samples that failed through the weld area under shear that were not included in this study due to poor weld quality. This data comes from Pekoz's earlier 1973 report co-authored by Yarnell, which is referenced in the 1979 report as Reference 5. Pekoz describes these poor quality welds in the 1979 report, "It should be noted that all of the field welded arc spot welds reported in Reference 5 were poorly made". The lack of quality of this data is evident when compared to Pekoz's other 24 weld shear failure samples not from Reference 5. When analyzed with Equation 1-1, the 1973 data resulted in a measured to predicted strength ratio of 0.983 and a coefficient of variation equal to 0.295, while the other 24

33

Pekoz samples resulted in 1.208 and 0.218 respectively. To maintain accuracy, arc spot weld data from Pekoz's 1973 report were excluded from this study.

In the analysis of Equation 1-1, this study carefully looked at Equation 1-5 (AISI S100-12 E2.2.2.1-5) which calculates the effective weld diameter, d_e, a major component of Equation 1-1. Easterling and Snow, Peuler, and Guenfoud noted that Equation 1-5 appeared to be conservative when compared to measured effective weld areas. Guenfoud developed Figure 3.2 to point out that Equation 1-5 is particularly conservative for specimens created with thicker combined sheet thicknesses. He recommends imposing a lower limit of $0.4d_{vis}$ to Equation 1-5 to improve the accuracy for samples with thicker combined thickness. This study explores a lower limit for Equation 1-5 and its effects on predicted weld shear strength (Equation 1-1) and predicted weld tension strength (Equation 1-7). The data analyzed for Equation 1-1 is presented in Table A-1 of Appendix A.
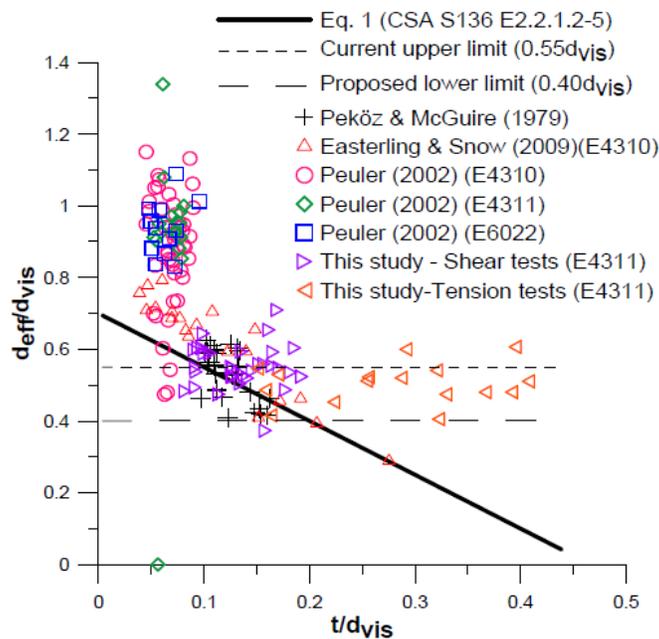
Figure 3.2: Figure 4.12 from Guenfoud's report of effective weld diameter results (Guenfoud, 2010).

34

Shear: Sheet Failure

Contributing authors included Pekoz, Peuler, Snow and Guenfoud for a total of 104 samples applicable to Equation 1-2 (AISI S100-12 E2.2.2.1-2), where d_a/t is less than $0.815\sqrt{(E/F_u)}$. This equation predicts the load at which sheet failure will occur for samples that have a larger design thickness, t, and smaller average weld diameters, d_a. Out of Guenfoud's 42 sheet shear failures, 34 of these were governed by Equation 1-2 as expected, since he contributed mostly 2 and 4 sheet thick welds. Peuler contributed 44 samples of a single sheet thickness and Snow provided 22 full-time weld samples of both one and two sheet thicknesses into this d_a/t range.

Pekoz, at first glance contributed many samples into this range, but unfortunately some had to be excluded. His 1979 report summarizes hundreds of weld specimens tested under his supervision at Cornell University, and references data from five reports he co-authored between 1971 and 1978. When dissecting the data presented in the 1979 report, this study found several cases where the data in the 1979 report did not match up with the original references. For example, consider Table 5 from the 1979 report pictured here in Figure 3.3. The ultimate stress of samples listed from the highlighted "Reference 4", correspond to specimens tested in a 1971 report titled "Tests on Puddle and Fillet Weld Connections" by Dhalla and Pekoz. Looking at Figure 3.3, sample A A/B 18/7 D1 is reported having a measured ultimate tensile stress of 67 ksi, but when observing Figure 3.4, picturing Table 2B from the original 1971 report, the same sample is reported having a measured ultimate tensile stress of 64.4 ksi.

Table 5. Arc Spot (Puddle) Welds: Summary of Results

1	2	3	4	5	6	7	8	9	10	11	12	13	14	15	16	17	18
	Measured and Computed Properties							Test Results		Predicted Results							
	Cover Plate					Weld				Cover Plate Results				Weld Failure			$\dfrac{P_{uo}}{P_{up}}$
Specimen Designation	σ_y ksi	σ_u ksi	S_{av} in	e_{av} in	t_{av} in	Visible Diam. in	Ave. Net Diam. of Sheared Welds in	P_{uo} kips	Failure Mode	d_a/t	$\dfrac{240}{\sqrt{\sigma_u}}$	P_u Eqn. 8	P_u Eqn. 9a	d_{en} in Eqn. 6	P_u Eqn. 7	Failure Mode	
Single Sheet Puddle Welds																	
Shop Welded Specimens (Reference 4)																	
A A/B 18/7 D1	48.92	67.0	3.50	1.40	0.049	0.79	–	13.48	PC+PL+PT	15.12	29.32	10.70	–	0.48	16.25	PC+PT	1.20
A A/B 18/7 D2	48.92	67.0	3.48	1.60	0.050	0.80	–	12.40	PC+PL+PT	15.00	29.32	11.06	–	0.49	16.63	PC+PT	1.12
A A/B 18/7 D3	48.92	67.0	3.49	1.60	0.049	0.81	–	13.10	PC+PL+PT	15.53	29.32	10.99	–	0.49	17.11	PC+PT	1.19
A A/B 18/7 D4	48.92	67.0	3.50	1.50	0.050	0.85	–	14.40	PC+PL+PT	16.00	29.32	11.79	–	0.52	19.11	PC+PT	1.22
A A/B 28/7 C1	109.8	109.8	3.50	1.45	0.016	0.64	–	2.76	PS+PB	39.00	22.90	–	3.07	0.42	12.71	PS+PB	0.90
A A/B 28/7 C2	109.8	109.8	3.48	1.45	0.016	0.64	–	1.94	PS+PB	39.00	22.90	–	3.07	0.42	12.71	PS+PB	0.63
A A/B 28/7 C3	109.8	109.8	3.48	1.45	0.016	0.57	–	2.60	PS+PB	34.63	22.90	–	2.73	0.38	9.94	PS+PB	0.95
A A/B 28/7 C4	109.8	109.8	3.50	1.40	0.016	0.59	–	2.54	PS+PB	35.88	22.90	–	2.82	0.39	10.70	PS+PB	0.90
A A/B 28/7 C5	109.8	109.8	3.47	1.40	0.016	0.56	–	2.72	PS+PB	34.00	22.90	–	2.68	0.37	9.57	PS+PB	1.01

Figure 3.3: View of Table 5 from Pekoz's 1979 report (Pekoz, 1979).

TABLE 2B

```
****************************
*      G R O U P   A        *
* SINGLE SHEET PUDDLE WELD  *
****************************
. . . . . . . . . . . . . . . . . . . . . .
.                                          .
.     EXPERIMENTAL    DATA                  .
.                                          .
. . . . . . . . . . . . . . . . . . . . . .
```

1	2	3	4	5	6	7	8	9	10	11	12	13	14	15
		AV. MATERIAL PROPS.			E X P E R I M E N T A L R E S U L T S									
SPECIMEN DESIGNATION	AREA OF CRITICAL SECTION	YLD. STR. (COVER PLATE)	ULT. STR. (COVER PLATE)	SHEAR STR. OF WELD	L O A D S			S T R E S S E S			DEF. AT		MODE OF FAILURE	FAILURE OBSERVED IN PLATE
					YIELD	ULT.	FINAL	YIELD (COVER PLATE)	ULT. (WELD)	SHEAR (WELD)	ULT. LOAD	FINAL LOAD		
	A_c SQ.IN.	σ_y KSI.	σ_t KSI.	τ_{sa} KSI.	P_y KIPS.	P_{ult} KIPS.	P_f KIPS.	σ_{yt} KSI.	σ_{tt} KSI.	τ_{su} KSI.	S_u IN.	δ_f IN.	TYPE	
A A/B 18/7 D1	0.357	47.00	64.40	39.20	11.40	13.48	2.00	32.0	37.8	–	0.35	0.75	PC+PL+PT	A+C
A A/B 18/7 D2	0.358	47.00	64.40	39.20	12.40	12.40	4.00	34.6	34.6	–	0.02	0.60	PC+PL+PT	B+D
A A/B 18/7 D3	0.356	47.00	64.40	39.20	11.50	13.10	2.00	32.3	36.8	–	0.35	0.80	PC+PL+PT	A+C
A A/B 18/7 D4	0.360	47.00	64.40	39.20	12.70	14.40	2.00	35.3	40.0	–	0.32	0.90	PC+PL+PT	A+D
A E/B 28/7 C1	0.126	97.60	97.60	39.20	2.76	2.76	R	21.9	21.9	–	0.02	0.70	PS+PB	A+D
A E/B 28/7 C2	0.125	97.60	97.60	39.20	P	1.94	0.40	P	15.5	–	0.03	0.80	PS+PB	B+C
A E/B 28/7 C3	0.125	97.60	97.60	39.20	2.60	2.60	0.80	20.8	20.8	–	0.02	0.70	PS+PB	A+D
A E/B 28/7 C4	0.126	97.60	97.60	39.20	P	2.54	0.80	P	20.2	–	0.01	0.60	PS+PB	B+D
A E/B 28/7 C5	0.175	97.60	97.60	39.20	P	2.72	0.80	P	21.8	–	0.05	0.50	PS+PB	B+C

Figure 3.4: View of Table 2B from Dhalla and Pekoz's 1971 report (Dhalla, 1971).

This type of reporting error was found multiple times throughout Pekoz's 1979 report, therefore this study took data directly from the original references in order to improve the accuracy of the analysis. Pekoz's 1979 report referenced data from "Tests on Puddle Weld Connections" by Fraczek and Pekoz, an unpublished letter report from 1975. Unfortunately, the original "Tests on Puddle Weld Connections" could not be located and this study excluded its

data into avoid misreported values found in the 1979 report. The exclusion of Fraczek's data left four remaining specimens from Pekoz in this d_a/t range for our analysis. Data pulled for analysis of Equation 1-2 is listed in Table A-4 of Appendix A.

Equation 1-3 (AISI S100-12 E2.2.2.1-3) predicts shear strength for specimens in the intermediate d_a/t range. Excluding 26 samples from Fung with unknown F_u values and the poor weld quality samples from the 1979 Pekoz report this study was left with 23 specimens to analyze in this range. Snow provided 11 specimens, Guenfoud contributed eight, while Peuler contributed four for analysis of Equation 1-3. Data contributed to Equation 1-3 is available in Table A-5 of Appendix A. No new data was available to analyze Equation 1-4 (AISI S100-12 E2.2.2.1-4), which predicts shear strength for the higher range of d_a/t. The study Recalibrated the resistance and safety factors using Pekoz's 1979 data, from which Equation 1-4 was originally derived. Only five samples met the range of $d_a/t \geq 1.397 \sqrt{(E/F_u)}$ for the entire data base.

Tension: Weld Failure

Within the existing data base for arc spot welds only Guenfoud was able to produce tension loaded specimens that experienced failure through the weld metal, which the resistance is calculated with Equation 1-7 (AISI S100-12 E2.2.3-1). LaBoube and Yu had tension weld failures but only for specimens that were welded with weld washers. Guenfoud reported an average a test to predicted strength ratio of 0.50 for his 16 tension weld failure samples, which was calculated applying a lower limit for the effective weld diameter calculation equal to 0.4 times the visible weld diameter ($0.40d \leq d_e$) as mentioned above in the shear weld failure discussion. Guenfoud speculated in his 2010 report that the poor test results were due to concentrated stresses on the weld perimeter caused by large weld diameters and the absence of weld washers. Based on test results, Guenfoud recommended that the strength calculated by

Equation 1-7 be reduced by 50%. This study explored application of a lower limit for effective weld diameter as well as a reduction to Equation 1-7.

Tension: Sheet Failure

Tension load failure of the sheet around the weld perimeter is predicted by Equation 1-8 (AISI S100-12 E2.2.3-2). This baseline equation can apply to various sheet configurations, some of which AISI S100-12 applies a reduction to the Equation 1-8 calculated value. The simplest configuration is an interior weld of either a single sheet or of double sheets as illustrated in Figure 3.5. According to AISI S100-12, interior weld configurations do not require a strength reduction. Contributing authors for interior welds includes LaBoube, who tested 88 single sheet interior welds and 18 double sheet interior welds, as well as Guenfoud, who tested 15 single sheet interior welds. Fung also performed several tension tests, but as previously mentioned, the specimens that failed through the sheet were not included in this analysis do to the lack of provided measured F_u values.
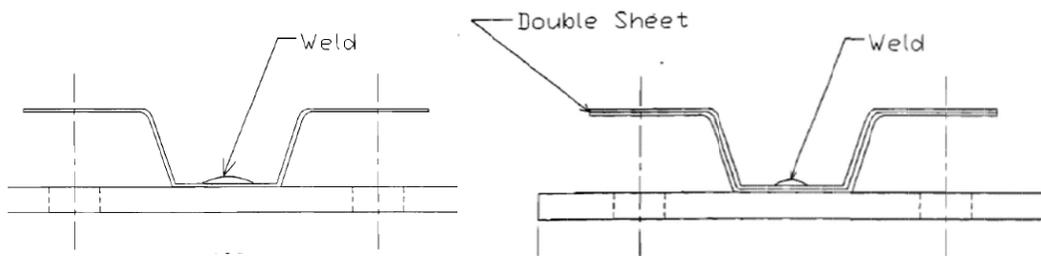
Figure 3.5: Interior weld configurations (LaBoube, 1991).

AISI S100-12 specifies a 50% reduction to the strength predicted by Equation 1-8 for welds exposed to eccentric loading. Eccentric tensile loading occurs on roofs where wind uplift stresses perimeter arc spot welds. In 1991 LaBoube tested 40 samples under eccentric loading to simulate wind uplift. The same test set up shown in Figure 2.10 was used, but only one side of the corrugated sheet steel was bolted to the test frame in order to induce an eccentric load

38

(illustrated in Figure 3.6). LaBoube limited eccentric loading to single sheet specimens. Although there have been no additional contributors to eccentric tensile loading since LaBoube's work, this study re-evaluates his data with Equation 1-8 and the 50% reduction.
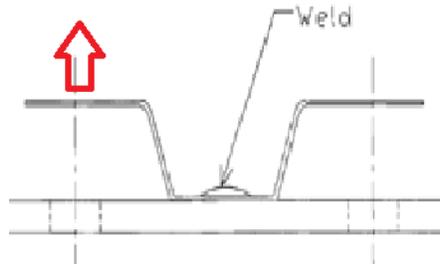
Figure 3.6: Eccentric tensile loading tested by LaBoube (LaBoube, 1991).

The final configuration for arc spot welds loaded in tension is a side-lap connection. This occurs when two sheets are welded together side by side, essentially the flange on the edge of one sheet is welded into the bottom of the edge corrugation of another. At the corners of four sheets connected together, a four layer side-lap occurs. Guenfoud tested 25 two sheet layer side-lap connections and 15 four sheet layer side-lap connections. These two configurations used by Guenfoud were previously presented in Figure 2.13. Currently AISI S100-12 applies a 30% reduction to the sheet tensile strength calculated by Equation 1-8.

LaBoube's 1991 report also tested two sheet layer side-lap connections. In LaBoube's study he varied how much the weld area overlapped the top flange. He called the amount of weld overlap, d′, as pictured to the right in Figure 2.11. LaBoube found that the amount of weld overlap played a significant role in the performance of the connection. This study includes only LaBoube's side-lap samples that had full weld coverage over the top flange. In other words, only samples whose d′ was equal to or greater than the full weld diameter were included. A total of 14 samples that met this criterion from LaBoube's work for this study.

Both Guenfoud and LaBoube noted in their reports that sheet failure always occurred through the top side-lap sheet (or sheets in the case of the four layer configuration), leaving the bottom lap intact. Therefore, both authors suggest to take the design thickness, t, used in Equation 1-8 and in Equation 1-5 for calculation of d_a as the thickness to the middle of the sheets. Therefore, in a two sheet side-lap connection, the design thickness should be equal to one sheet thickness. Likewise, in a four sheet side-lap connection, the design thickness should be equal to two sheet thicknesses. By taking the thickness as half of the total, now only the resistance of the top lap is considered, thereby accurately reflecting what happens during failure. Currently, this distinction in design thickness for side-lap connections is not specified by AISI S100-12. This study compares use of the full design thickness and the half thickness as recommended by Guenfoud and LaBoube.

Effective Weld Diameter

The calculation of effective weld diameter, Equation 1-5 (AISI S100-12 E2.2.2.1-5) was also analyzed in this study. Equation 1-5 was originally created by Pekoz, based on the measured effective weld diameter of his samples that failed by weld shear. Since Pekoz's work in the 1970's, other authors have contributed to measured effective weld diameter data base to include Snow and Easterling and Guenfoud. Equation 1-5, like the strength equations, was also re-evaluated with the comprehensive data base.

Analysis in the recent unpublished 2016 report, "Re-evaluation of AISI Effective Diameter Equations for Arc Spot Welds" by Kevin Church and Brian Bogh was the first to compare measured effective weld diameters of Pekoz with that of Snow and Easterling. This study assessed the analysis performed by Church and Bogh as well as incorporated data from Guenfoud for a full comprehensive evaluation of Equation 1-5.

Sheet Thickness

In addition to the evaluation of the arc spot weld strength equations and effective weld diameter calculation, this study also assessed the AISI S100-12 specification of a combined sheet thickness maximum of 0.15 inches (3.81 mm). When this specification was created, 0.15 inches was the thickest specimen in the data base. Today's expanded data base now includes arc spot welds through combined sheet thicknesses up to 0.23 inches (5.84 mm) by Guenfoud. Guenfoud was able penetrate through thicker sheets by use of an E6011 electrode to maximize weld penetration. The combined sheet thicknesses ranged from 0.092 inches (2.34 mm) to 0.23 inches (5.84 mm) of Guenfoud's sixteen tension samples that failed through the weld. This study assessed the performance of welds made through sheets below the current 0.15 inch limit and the above it in order to evaluate the maximum limit.

Calculation of Resistance and Safety Factors

Once data was collected from contributing authors it was analyzed in accordance to AISI 2012 section F1.1 to determine resistance and safety factors, ϕ and Ω for LRFD, ASD and LSD. The target reliability index, β, defines how conservative the resistance and safety factors will be. This study performed calculations with a reliability index of 3.5 for LRFD and ASD shear equations, and both 3.5 and 3.0 for tension equations as specified by AISI S100-12. When calculating resistance factors for LSD, the reliability index was changed to 4.0 and 3.5, respectively as specified for connections by section F1.1. To calculate safety factors for ASD, this study used a ratio with the LRFD resistance factor of 1.53/ϕ. This ratio is consistent with safety factors listed in AISI S100-12 and it correlates with a live to dead load ratio equal to 5.0. All variables and coefficients selected for the calculation of the resistance and safety factors were with respect to section F1.1 and are presented for each AISI equation analyzed in Appendix B.

41

CHAPTER 4
RESULTS

Effective Weld Diameter

The calculation for effective weld diameter, d_e, Equation 1-5 (AISI S100-12 E2.2.2.1-5) was evaluated with measured effective weld diameters gathered from reports by Pekoz, Snow and Easterling, and Guenfoud. Church and Bogh performed an interesting analysis, assessing the origin of the current maximum listed in Equation 1-5, 0.55d. Consider Figure 4.1, which plots Pekoz's data of measured effective weld diameters. The blue line represents the best fit equation, the red line is the published equation, E2.2.2.1-5, and the green line depicts the current 0.55d effective weld diameter maximum. Church and Bogh point out in their report that the 0.55d maximum was likely incorporated into AISI S100-12 E2.2.2.1-5 due to lack of additional data in the lower ranges of t/d horizontal axis of Figure 4.1.
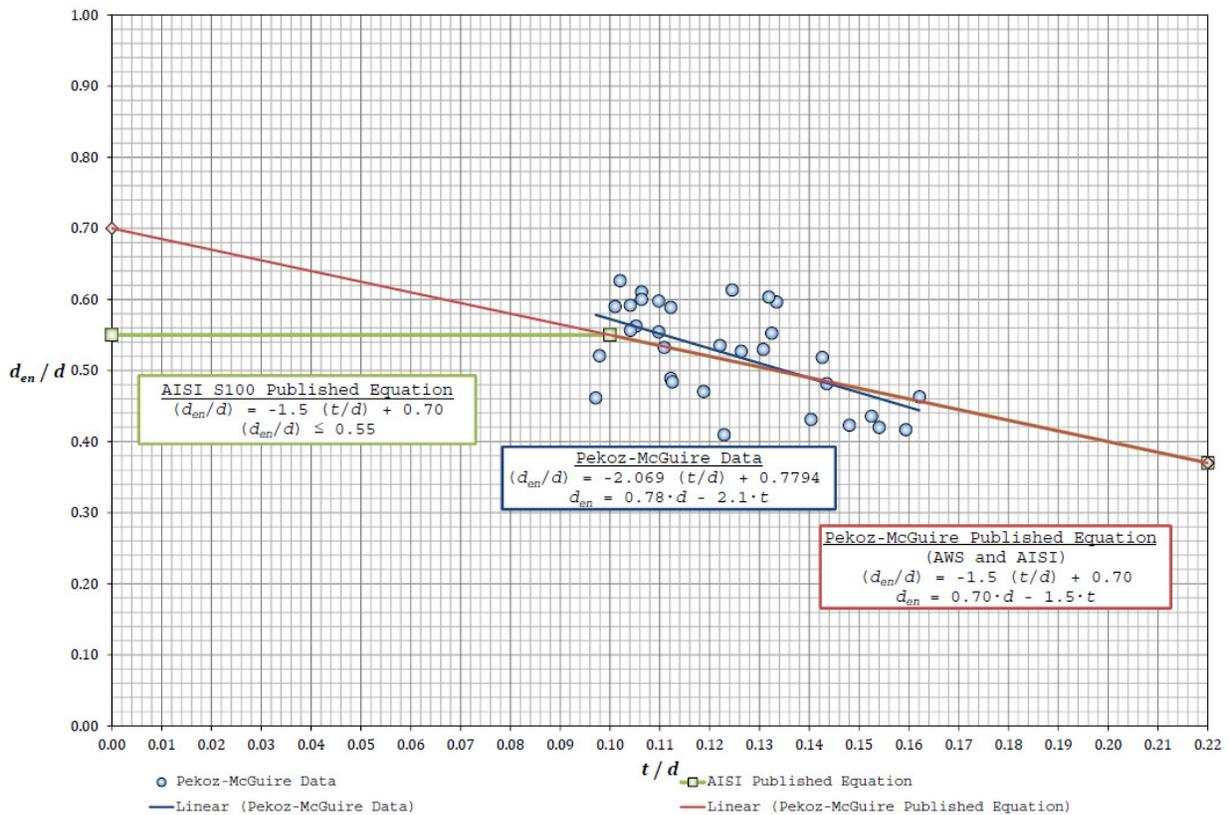
Figure 4.1: Evaluation of effective weld diameter with Pekoz data (Church, 2016).

42

In 2008, Snow and Easterling expanded the effective weld diameter data base by sectioning arc spot weld connections after shear testing. Once sectioned, the effective, visual, and average weld diameters were measured. Snow and Easterling's data populated lower ranges of t/d (horizontal axis) as demonstrated in Church and Bogh's graph in Figure 4.2. Comparing Figure 4.1 with Figure 4.2, it is apparent that the 0.55d maximum (green line) does not represent Snow and Easterling's data. Rather, Snow and Easterlings data continues the trend line of Pekoz's data. Combined, the data is best represented by the black line in Figure 4.2, which is similar to Equation 1-5 but doesn't include a maximum limit.

FIGURE 1-3: EFFECTIVE DIAMETER - AISI vs. Pekoz-McGuire vs. Combined Data Equation

Combined Data
$(d_{en}/d) = -1.292 \ (t/d) + 0.7112$
$d_{en} = 0.71 \cdot d - 1.3 \cdot t$

AISI S100 Published Equation
$(d_{en}/d) = -1.5 \ (t/d) + 0.70$
$(d_{en}/d) \leq 0.55$

Pekoz-McGuire Published Equation
(AWS and AISI)
$(d_{en}/d) = -1.5 \ (t/d) + 0.70$
$d_{en} = 0.70 \cdot d - 1.5 \cdot t$

○ Pekoz-McGuire Data   ▫ AISI Published Equation
△ Snow-Easterling   — Linear (Pekoz-McGuire Published Equation)
— Linear (Combined Data)

Figure 4.2: Evaluation of effective weld diameter with combined data from Pekoz and Snow and Easterling (Church, 2016).

Expanding the analysis performed by Church and Bogh, this study also incorporated effective weld diameters measured by Guenfoud which populated higher ranges of the t/d

43

horizontal axis. The comprehensive data from all three reports is presented in Figure 4.3. Note, that this study only considered data from full time welded specimens for the Snow and Easterling report.
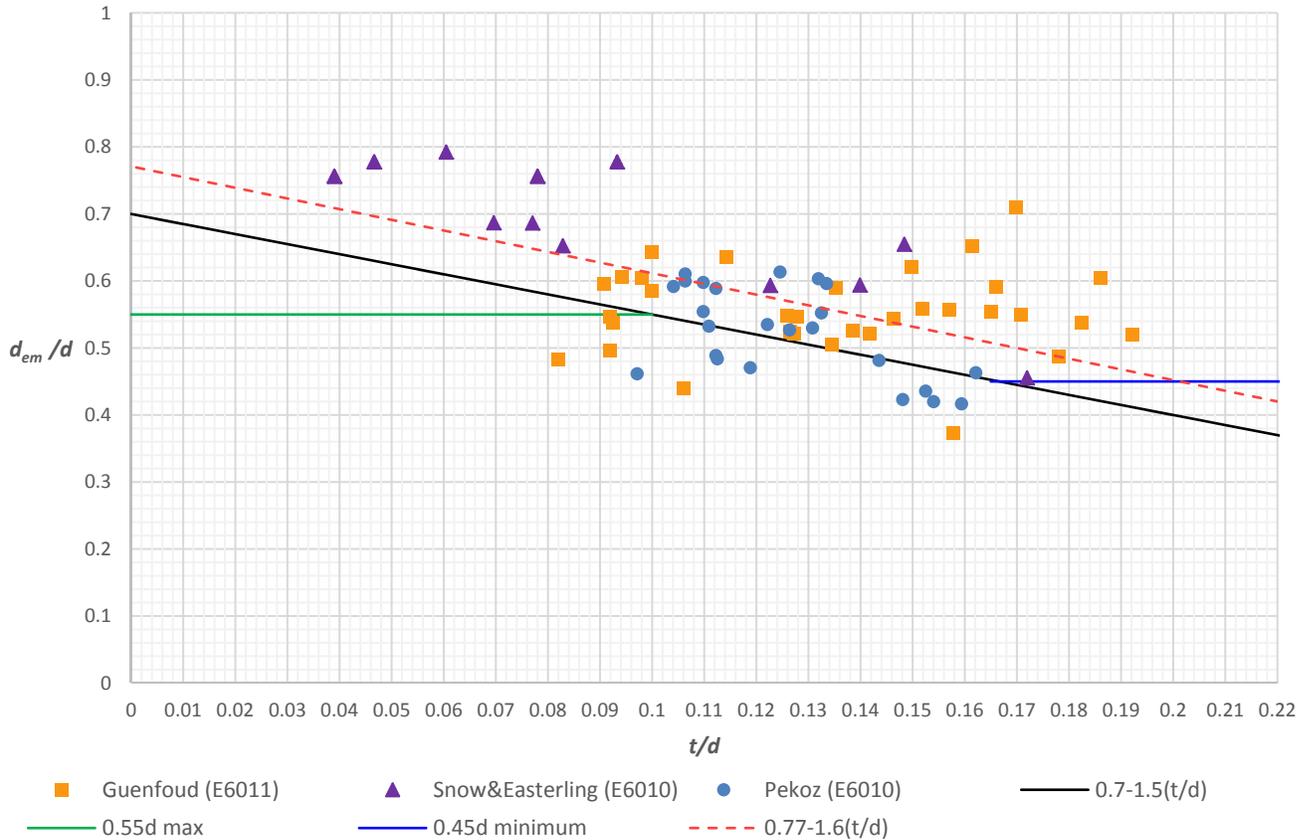
Figure 4.3: Evaluation of effective weld diameter with data from Pekoz, Snow and Easterling, and Guenfoud.

The black lines represent the Equation 1-5 (AISI S100-12 E2.2.2.1-5), and the green line represents the current 0.55d maximum. With the addition of Snow and Easterling's and Guendfoud's data it is apparent that the 0.55d maximum is not representative of the measured effect weld diameters in this range and therefore the maximum should be removed. It is also observed on the larger ranges of t/d that the black line (current equation) under predicts effective weld diameters. One solution would be to incorporate a lower limit equal to 0.45d, represented

by the blue line. With these changes, Equation 1-5 would evolve to Equation 4-1, represented by the black and blue lines in Figure 4.3.

$$d_e = \text{greater of} \quad 0.7d - 1.5t \qquad\qquad\qquad (\text{Eq. 4-1})$$
$$0.45d$$

An alternative would be to use the best fit linear equation for the comprehensive data set represented by the red dashed line. By updating the equation, it is possible that no limits are necessary. The linear equation that best represents the combined data is presented in Equation 4-2. Ultimately it will be up to the AISI committee which approach they believe is best, but it is apparent that E2.2.2.1-5 needs to be upgraded to represent the improved comprehensive data base since Pekoz's work. Weld fracture strength Equations 1-1 (shear) and 1-7 (tension) are evaluated using both the current equation for effective weld diameter and the proposed Equations 4-1 and 4-2.

$$d_e = 0.77d - 1.6t \qquad\qquad\qquad\qquad (\text{Eq. 4-2})$$

Interestingly, Guenfoud was able to weld through very thick combined sheets up to 0.23 inches (5.84 mm) total by using an E6011 electrode, which proved to have the best penetration
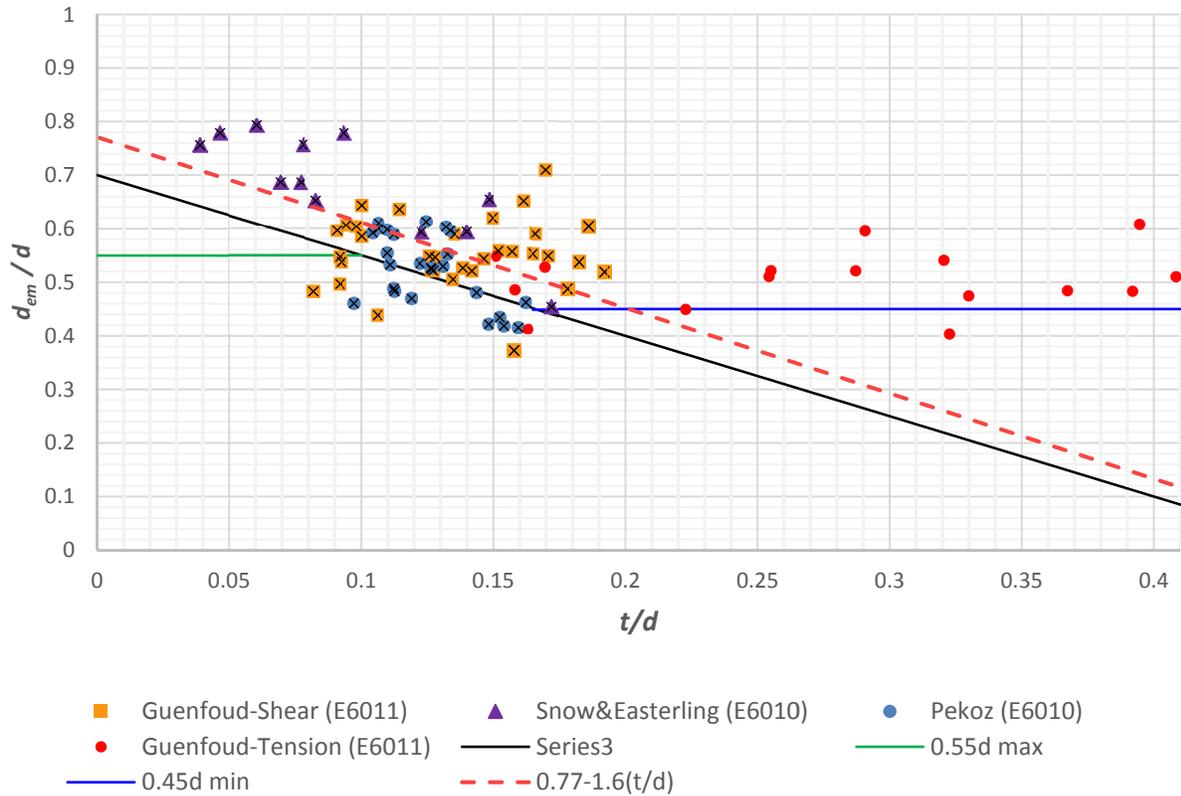
capabilities in both Peuler and LaBoube's reports. Guenfoud's tension weld failure specimens also had their effective diameters measured after tension failure and are included in Figure 4.4. The red dots on the graph are Guenfoud's tension weld specimens and as mentioned earlier, are the only specimens in the data base that failed in this manner without use of weld washers. Its apparent this is because he was able to weld through thicker sheets than any previous author. For Guenfoud's tension samples it appears that the 0.45d lower limit (blue line) is a much better fit than either Equation 1-5 or Equation 4-2, which severely under predict these effective weld diameters. The effect of each d_e calculation method on Equation 1-7, governing these tension weld failures is assessed in sections below.

Figure 4.4: Evaluation of effective weld diameter including Guenfoud's tension data.

Shear: Weld Failure

The current equation for weld shear strength in an arc spot welded connection, Equation 1-1 (AISI S100-12 E2.2.2.1-1), was analyzed with 87 samples contributed by Guenfoud, Snow, Pekoz, and Fung. The effective weld diameter, d_e, inserted into Equation 1-1 was calculated with Equation 1-5 (AISI S100-12 E2.2.2.1-5) and proposed Equations 4-1 and 4-2. Each d_e calculation method was compared to see which produced the most accurate Equation 1-1 strength prediction. Observing Table 4-1, it appears there is little difference in the performance of the current AISI d_e Equation 1-5 and the proposed d_e Equation 4-1. Both result in a LFRD resistance factor close to 0.60, matching what is currently specified in AISI S100-12. This illustrates that removing the upper limit on d_e, of 0.55d has little to no effect on the accuracy of Equation 1-1.

Interestingly, the best fit equation for d_e, Equation 4-2, had the weakest performance when applied to Equation 1-1 as presented in the right column of Table 4-1. Equation 4-2 also produced the lowest test to predicted strength ratio equal to 1.23 when compared to 1.56 and 1.53 of Equations 1-5 and 4-1 respectively. So, why would Equation 4-2 be the best fit of effective weld diameter data but not the shear weld failure specimen data? The explanation is rooted in specimens sectioned by Snow and Easterling which populated lower ranges of the t/d axis in Figure 4.3. These specimens had larger diameter welds with respect to their combined sheet thickness and thereby actually failed through the sheet rather than through the weld. Snow's data pulls the best fit line for d_e (the dashed red line in Figure 4.3) up from the current Equation 1-5 (the black line in Figure 4.3) and truly is the best fit for effective weld diameters of all ranges. But, Equation 1-1 is re-evaluated only with specimens that failed via weld shear, which doesn't include specimens that had to be sectioned to measure effective weld diameters.

47

Therefore, Equation 1-1 data is best represented by a d_e calculation that represents those samples that fail in weld shear, closer to $d_e = 0.7d\text{-}1.5t$ as used in Equation 1-5 and 4-1. Note that all Recalibrated values are provided with four significant figures in the results tables. All recommendations will be provided with three significant figures.

Table 4-1: Equation 1-1 (E2.2.2.1-1) existing and Recalibrated resistance and safety factors.

Design Factor	Existing	Recalibrated with AISI S100-12 d_e	Recalibrated with Equation 4-1 d_e	Recalibrated with Equation 4-2 d_e
ϕ (LRFD, $\beta = 3.5$)	0.60	0.595	0.591	0.472
Ω (ASD, $\beta = 3.5$)	2.55	2.571	2.587	3.243
ϕ (LSD, $\beta = 4.0$)	0.50	0.450	0.448	0.356
No. of Samples = 87				

Although there is not a profound difference with removing the upper limit of 0.55d and adding the lower limit of 0.45d for shear weld failure data presented in Table 4-1, there is significant improvement for the tension weld failure data as explained in the Equation 1-7 analysis below. Applying Equation 4-1, Equation 1-1 reached a measured to predicted strength ratio of 1.53 and a coefficient of variation equal to 0.326.

Shear: Sheet Failure

Equation 1-2 (AISI S100-12 E2.2.2.1-2) characterizes sheet failure for samples with a smaller weld diameter compared total sheet thickness. After a detailed data analysis following the AISI S100 section F1.1 specifications for calculation of resistance and safety factors for arc spot welded connections as detailed above the existing equation was found to be an accurate prediction sheet shear strength. No change is recommended to Equation 1-2, but resistance and safety factors improved when considering applicable specimens from the entire data base as presented in Table 4-2. From 104 specimens, Equation 1-2 produced an average test to predicted

strength ratio of 1.41 and a coefficient of variation equal to 0.182. The existing and recalibrated resistance and safety factors for Equation 1-2 are provided in Appendix B.

Table 4-2: Equation 1-2 (E2.2.2.1-2) existing and Recalibrated resistance and safety factors.

Design Factor	Existing	Recalibrated
ϕ (LRFD, $\beta = 3.5$)	0.70	0.787
Ω (ASD, $\beta = 3.5$)	2.20	1.943
ϕ (LSD, $\beta = 4.0$)	0.60	0.629
No. of Samples = 104		

Equation 1-3 (AISI S100-12 E2.2.2.1-3) characterizes sheet failure of specimens in the intermediate range of d_a/t. After analysis of 23 samples from Guenfoud and Peuler and Snow, Equation 1-3 was found to adequately predict the shear connection strength of arc spot welded samples. No change is recommended to Equation 1-3, but resistance and safety factors improved when considering applicable specimens from the entire data base. Equation 1-3 produced an average test to predicted strength ratio of 1.40 and a coefficient of variation equal to 0.122. The existing and recalibrated resistance and safety factors for Equation 1-3 are provided in Table 4-3 below.

Table 4-3: Equation 1-3 (E2.2.2.1-3) existing and Recalibrated resistance and safety factors.

Design Factor	Existing	Recalibrated
ϕ (LRFD , $\beta = 3.5$)	0.55	0.865
Ω (ASD , $\beta = 3.5$)	2.80	1.770
ϕ (LSD , $\beta = 4.0$)	0.45	0.700
No. of Samples = 23		

Although there was no additional data after the Pekoz 1979 report to analyze Equation 1-4 (AISI S100-12 E2.2.2.1-4), this study Recalibrated the resistance and safety factors with Pekoz's five applicable samples. The results are presented in Table 4-4. After this analysis, no change to Equation 1-4 is recommended and the existing resistance and safety factors appear to

be adequate. The average test to predicted strength ratio is 0.99 and the coefficient of variation

is equal to 0.167.

Table 4-4: Equation 1-4 (E2.2.2.1-4) existing and Recalibrated resistance and safety factors.

Design Factor	Existing	Recalibrated
ϕ (LRFD, $\beta = 3.5$)	0.50	0.467
Ω (ASD, $\beta = 3.5$)	3.05	3.279
ϕ (LSD, $\beta = 4.0$)	0.40	0.364
No. of Samples = 5		

Tension: Weld Failure

The current tension weld strength equation, Equation 1-7 (AISI S100-12 E2.2.3-1) was

analyzed with 16 samples from Guenfoud. Note that the data base analyzed for Equation 1-7

does not include specimens welded with weld washers. Other authors induced tension weld

failures in their specimens but only Guenfoud was able to do so without weld washers. He was

able to reach tension weld failure without use of a weld washer by welding through combined

sheet thicknesses up to 0.23 inches (5.84 mm) thick. Equation 1-7 was evaluated using the

current specified calculation for effective weld diameter, d_e, Equation 1-5 (AISI S100-12

E2.2.2.1-5) as well as proposed Equations 4-1 and 4-2. It appears Equation 1-7 is not

representative of Guenfoud's data when applying Equation 1-5 or 4-2, as illustrated in the

"Recalibrated" columns in Table 4-5 and Table 4-6. The issue is that Equation 1-5 and Equation

4-2 severely under calculate the effective weld diameter of specimens with thicker combined

sheet thicknesses. Equation 1-5 averaged a computed to measured effective weld diameter ratio

equal to an average of 0.56 for Guenfoud's 16 specimens. This under representation of effective

weld diameter resulted in an equally poor coefficient of variation (COV) for Equation 1-7 equal

to 1.43.

By applying a lower limit for d_e equal to 0.45d as shown in Equation 4-1, the computed to measured diameter ratio improved to 0.91 and the COV for Equation 1-7 sharpened to 0.362. Even with the improved COV by using Equation 4-1, Equation 1-7 still produced a measured to predicted strength ratio of 0.62. In order to bring this ratio above 1.0, this study agrees with the recommendation from Guenfoud's report to introduce a reduction to Equation 1-7 of 0.50. The reduction should only be applied to welds without weld washers. By doing so, the strength ratio improves to 1.24 and the resistance and safety factors in the fourth columns of Table 4-5 and Table 4-6 are produced. Note that "r" equals the coefficient to reduce predicted strength by 50%.

Table 4-5: Equation 1-7 (E2.2.3-1) existing and Recalibrated resistance and safety factors for eccentric tensile loading using lower β (panel and deck).

Design Factor	Existing	Recalibrated with AISI S100-12 d_e	Recalibrated with **Equation 4-1** d_e and r =0.50	Recalibrated with Equation 4-2 d_e and r =0.50
φ (LRFD, β = 3.0)	0.60	0.062	**0.499**	0.115
Ω (ASD, β = 3.0)	2.50	24.677	**3.066**	13.312
φ (LSD, β = 3.5)	0.50	0.026	**0.368**	0.051
No. of Samples = 16				

Table 4-6: Equation 1-7 (E2.2.3-1) existing and Recalibrated resistance and safety factors for eccentric tensile loading using higher β (other).

Design Factor	Existing	Recalibrated with AISI S100-12 d_e	Recalibrated with **Equation 4-1** d_e and r =0.50	Recalibrated with Equation 4-2 d_e and r =0.50
φ (LRFD, β = 3.5)	0.50	0.028	**0.394**	0.055
Ω (ASD, β = 3.5)	3.00	54.643	**3.887**	27.897
φ (LSD, β = 4.0)	0.40	0.012	**0.290**	0.024
No. of Samples = 16				

Tension: Sheet Failure

Equation 1-8 (AISI S100-12 E2.2.3-2) was analyzed separately for interior, eccentrically loaded, and side-lap data. One and two sheet interior weld configurations were contributed by LaBoube and Guenfoud, for a total of 121 specimens. For tension loading, AISI S100-12 specifies two connection categories: either panel and deck applications or all other applications. The difference between these categories is their specified reliability indexes (β) for the calculation of resistance and safety factors. For panel and deck applications the reliability index (β) used to calculation the resistance and design factors is 3.0 (U.S.), while for all other applications it is 3.5 (U.S.) Existing and Recalibrated resistance and safety factors for combined interior configurations for both reliability indexes are presented in Table 4-7 Table 4-8. The average test to predicted strength ratio is 1.27 and the coefficient of variation is equal to 0.223.

Table 4-7: Equation 1-8 (E2.2.3-2) existing and Recalibrated resistance and safety factors for interior weld configurations using a lower β (panel and deck).

Design Factor	Existing	Recalibrated
ϕ (LRFD, β = 3.0)	0.60	0.767
Ω (ASD, β = 3.0)	2.50	1.994
ϕ (LSD, β = 3.5)	0.50	0.605
No. of Samples = 121		

Table 4-8: Equation 1-8 (E2.2.3-2) existing and Recalibrated resistance and safety factors for interior weld configurations using a higher β (other).

Design Factor	Existing	Recalibrated
ϕ (LRFD, β = 3.5)	0.50	0.648
Ω (ASD, β = 3.5)	3.00	2.363
ϕ (LSD, β = 4.0)	0.40	0.511
No. of Samples = 121		

Eccentrically tensile loaded samples from LaBoube's 1991 report were also evaluated under Equation 1-8 and AISI S100-12 specified 50% reduction for eccentric configurations. A

total of 40 single sheets were evaluated in this study for panel and deck applications ($\beta = 3.0$, U.S.) and all other applications ($\beta = 3.5$, U.S.). Under the AISI S100-12 specification, the eccentrically loaded data analysis resulted in a tested to predicted strength ratio of 1.27 and a coefficient of variation equal to 0.278. Equation 1-8 and the 50% reduction appear to work well for eccentrically loaded arc spot welds, although the Recalibrated resistance and safety factors have been slightly improved from what is currently specified in AISI S100-12 as observed in Table 4-9 and Table 4-10. Note that "r" equals the coefficient to reduce predicted strength by 50%.

Table 4-9: Equation 1-8 (E2.2.3-2) existing and Recalibrated resistance and safety factors for eccentric tensile loading using lower β (panel and deck).

Design Factor	Existing (r = 0.50)	Recalibrated (r = 0.50)
ϕ (LRFD, β = 3.0)	0.60	0.669
Ω (ASD, β = 3.0)	2.50	2.287
ϕ (LSD, β = 3.5)	0.50	0.516
No. of Samples = 40		

Table 4-10: Equation 1-8 (E2.2.3-2) existing and Recalibrated resistance and safety factors for eccentric tensile loading using higher β (other).

Design Factor	Existing (r = 0.50)	Recalibrated (r = 0.50)
ϕ (LRFD, β = 3.5)	0.50	0.552
Ω (ASD, β = 3.5)	3.00	2.772
ϕ (LSD, β = 4.0)	0.40	0.426
No. of Samples = 40		

Side-lap configurations studied include two sheet laps and four sheet laps, pictured in Figure 2.13 contributed from Guenfoud and LaBoube. Interestingly, the four layer sheets performed much better than the two layer sheets. This is likely due to the increased stiffness of the thicker two top laps, thereby reducing the peeling effect around the weld perimeter. Using a design thickness equal to the uppermost sheet thickness as recommended by Guenfoud and

LaBoube the results for two sheet and four sheet side-laps are presented in Table 4-11 through Table 4-14. A test to predicted strength ratio of 1.51 and a coefficient of variation of 0.313 were achieved for two sheet side-laps, while a test to predicted strength ratio of 1.31 and a coefficient of variation of 0.121 were attained for four sheet side-laps. AISI S100-12 specifies to reduce the predicted strength of side-lap connections by 30%. This reduction is represented by "r" in Equation 1-8. The reduction was first recommended by LaBoube in 1991.

Guenfoud points out that the reduction recommended by LaBoube was targeted at side-laps that did not have full weld coverage over the top lap. If only samples with full weld coverage are accepted, as done in this study, it is possible to use the full strength predicted by Equation 1-8. This effect on the Recalibrated design and safety factors is exhibited in the right columns of Table 4-11 through Table 4-14 where "r" equals 1.0, hence no reduction is applied. It can be observed that when no reduction is applied, the resistance and safety factors calculate to a reasonable value, therefore a reduction of 30% may no longer be necessary.

Table 4-11: Equation 1-8 (E2.2.3-2) existing and Recalibrated resistance and safety factors for TWO sheet side-lap connections using lower β (panel and deck, design thickness of 1/2 total thickness).

Design Factor	Existing (r = 0.70)	Recalibrated (r =0.70)	Recalibrated (r = 1.0)
ϕ (LRFD, β = 3.0)	0.60	0.758	0.530
Ω (ASD, β = 3.0)	2.50	2.018	2.887
ϕ (LSD, β = 3.5)	0.50	0.583	0.408
No. of Samples = 39			

Table 4-12: Equation 1-8 (E2.2.3-2) existing and Recalibrated resistance and safety factors for TWO sheet side-lap connections using higher β (other, design thickness of 1/2 total thickness).

Design Factor	Existing (r = 0.70)	Recalibrated (r =0.70)	Recalibrated (r = 1.0)
φ (LRFD, β = 3.5)	0.50	0.624	0.437
Ω (ASD, β = 3.5)	3.00	2.452	3.501
φ (LSD, β = 4.0)	0.40	0.480	0.336
No. of Samples = 39			

Table 4-13: Equation 1-8 (E2.2.3-2) existing and Recalibrated resistance and safety factors for FOUR sheet side-lap connections using lower β (panel and deck, design thickness of 1/2 total thickness).

Design Factor	Existing (r = 0.70)	Recalibrated (r =0.70)	Recalibrated (r = 1.0)
φ (LRFD, β = 3.0)	0.60	0.927	0.649
Ω (ASD, β = 3.0)	2.50	1.650	2.357
φ (LSD, β = 3.5)	0.50	0.750	0.525
No. of Samples = 15			

Table 4-14: Equation 1-8 (E2.2.3-2) existing and Recalibrated resistance and safety factors for FOUR sheet side-lap connections using higher β (other, design thickness of 1/2 total thickness).

Design Factor	Existing (r = 0.70)	Recalibrated (r =0.70)	Recalibrated (r = 1.0)
φ (LRFD, β = 3.5)	0.50	0.803	0.562
Ω (ASD, β = 3.5)	3.00	1.905	2.722
φ (LSD, β = 4.0)	0.40	0.650	0.455
No. of Samples = 15			

The results of combined two and four sheet side-lap arc spot weld configurations are presented in Tables Table 4-15 Table 4-16. When combined, a test to predicted strength ratio of 1.46 and a coefficient of variation of 0.287 were reached. Data in Table 4-15 and Table 4-16 were computed using a design thickness equal to half of the total thickness as recommended by

55

Guenfoud and LaBoube while Table 4-17 Table 4-18 use a design thickness equal to the total sheet thickness as currently specified by AISI S100-12 for side-lap connections. Using the full combined sheet thickness, Equation 1-8 proves to over predict the strength of arc spot welded side-lap connections. This study could only reach the existing design and safety factors by reducing Equation 1-8 strength by 55%, as observed in the right columns of Table 4-17 and Table 4-18. Comparing the four tables and considering that sheet failure was observed only through the top lap by both Guenfoud and LaBoube it is very clear that using one half of the combined sheet thickness produces most accurate strength calculation for side lap configurations.

Table 4-15: Equation 1-8 (E2.2.3-2) existing and Recalibrated resistance and safety factors for COMBINED side-lap connections using lower β (panel and deck, design thickness of 1/2 total thickness).

Design Factor	Existing (r = 0.70)	Recalibrated (r =0.70)	Recalibrated (r = 1.0)
φ (LRFD, β = 3.0)	0.60	0.758	0.530
Ω (ASD, β = 3.0)	2.50	2.018	2.887
φ (LSD, β = 3.5)	0.50	0.583	0.408
No. of Samples = 54			

Table 4-16: Equation 1-8 (E2.2.3-2) existing and Recalibrated resistance and safety factors for COMBINED side-lap connections using higher β (other design thickness of 1/2 total thickness).

Design Factor	Existing (r = 0.70)	Recalibrated (r =0.70)	Recalibrated (r = 1.0)
φ (LRFD, β = 3.5)	0.50	0.624	0.437
Ω (ASD, β = 3.5)	3.00	2.452	3.501
φ (LSD, β = 4.0)	0.40	0.480	0.336
No. of Samples = 54			

Table 4-17: Equation 1-8 (E2.2.3-2) existing and Recalibrated resistance and safety factors for COMBINED side-lap connections using lower β and FULL thickness (panel and deck).

Design Factor	Existing (r = 0.70)	Recalibrated (r =0.70)	Recalibrated (r =0.50)	Recalibrated (r =0.45)
ϕ (LRFD, β = 3.0)	0.60	0.406	0.569	0.632
Ω (ASD, β = 3.0)	2.50	3.768	2.689	2.421
ϕ (LSD, β = 3.5)	0.50	0.312	0.436	0.485
No. of Samples = 54				

Table 4-18: Equation 1-8 (E2.2.3-2) existing and Recalibrated resistance and safety factors for COMBINED side-lap connections using higher β and FULL thickness (other).

Design Factor	Existing (r = 0.70)	Recalibrated (r =0.70)	Recalibrated (r =0.50)	Recalibrated (r =0.45)
ϕ (LRFD, β = 3.5)	0.50	0.333	0.467	0.519
Ω (ASD, β = 3.5)	3.00	4.595	3.276	2.948
ϕ (LSD, β = 4.0)	0.40	0.256	0.358	0.398
No. of Samples = 54				

Sheet Thickness Limitation

Guenfoud's sixteen tension weld failure specimens were split into those with a combined sheet thickness below the AISI S100-12 maximum of 0.15 inches (3.81 mm) and those above it. Of these specimens, six had a thickness less than 0.15 inches and ten had a thickness greater than 0.15 inches with a maximum of 0.23 inches (5.84 mm). Applying the previously recommended Equation 4-1 for calculation of effective weld diameter and Equation 1-7 (AISI S100-12 E2.2.3-1) with a 50% reduction, Table 4-19 compares the performance of samples below and above the current AISI S100-12 maximum thickness limit.

Table 4-19 demonstrates that samples between 0.15 inches and 0.25 inches do not drive down the performance of the tension weld strength calculation. Although the coefficient of variation is greater for thicker samples, the average measured to predicted strength ratio is larger

57

which provides a larger resistance factor. Therefore, samples above the maximum limit of 0.15 inches do not poison the results. It appears using an E6011 electrode proper penetration can still achieved through combined sheets thicker than 0.15 inches.

Table 4-19: Combined Sheet Thickness Comparison for Tension Weld Failures

	t ≤ 0.15"	0.15" < t < 0.25"	Combined t < 0.25"
Average (Pt/Pn)	0.956	1.407	1.238
COV	0.212	0.339	0.362
φ (LRFD)	0.497	0.564	0.499

The AISI S100-12 maximum thickness of 0.15 inches is applied to the total thickness of combined sheets. In the case of tension weld failure in Table 4-19, the total combined thickness is equal to the design thickness (the thickness to the plane of failure). In the case of tension weld failure the failure plane is between the combined sheets and the base metal. In other cases such as side laps, and non-perimeter multi-ply shear welds the failure plane is at the mid thickness of the combined sheets, therefore the design thickness is half of the total combined thickness. The arc-spot weld data base for side laps and various shear configurations include specimens that have a combined sheet thickness greater than 0.15 inches, but with a design thickness below 0.15 inches and yet still provided results that outperformed what is currently listed in AISI S100-12. Based on these results, it is of interest for AISI to increase the maximum combined thickness limit up to 0.23 inches for all arc spot welded connections.

CHAPTER 5

CONCLUSIONS AND RECOMMENDATIONS

The arc spot weld data base has drastically increased since LaBoube's work in 1991 by the work contributed by additional authors such as Peuler, Snow and Easterling, and Guenfoud. By combining the new data with old and by excluding select poor quality specimens as noted above the applicability of the existing AISI S100-12 arc spot design equations E2.2.2.1-1, E2.2.2.1-2, E2.2.2.1-3, E2.2.2.1-4, E2.2.2.1-5, E2.2.3-1 and E2.2.3-2 were assessed. Many design equations demonstrated improved performance under the enlarged data base, resulting in more favorable resistance and safety factors. This study also targeted equations and limitations that may need to be slightly altered in order to accurately predict arc spot weld connection strength.

Effective Weld Diameter

Equation 1-5 (AISI S100-12 E2.2.2.1-5) was assessed with new data from Snow and Easterling and Guenfoud in addition to Pekoz of which the orginal equation is based. Proposed Equations 4-1 and 4-2 were evaluated in comparison with Equation 1-5 and applied to data analysis of weld fracture Equations 1-1 (shear strength) and 1-7 (tension strength). Equation 4-1 by far was the best performer in all cases. This recommendation would remove the 0.55d maximum limit and add a 0.45d minimum limit. Not only does it produce the best results for Equations 1-1 and 1-7 but as presented in Figure 5.1 this change would represent the effective diameter data base quite nicely.
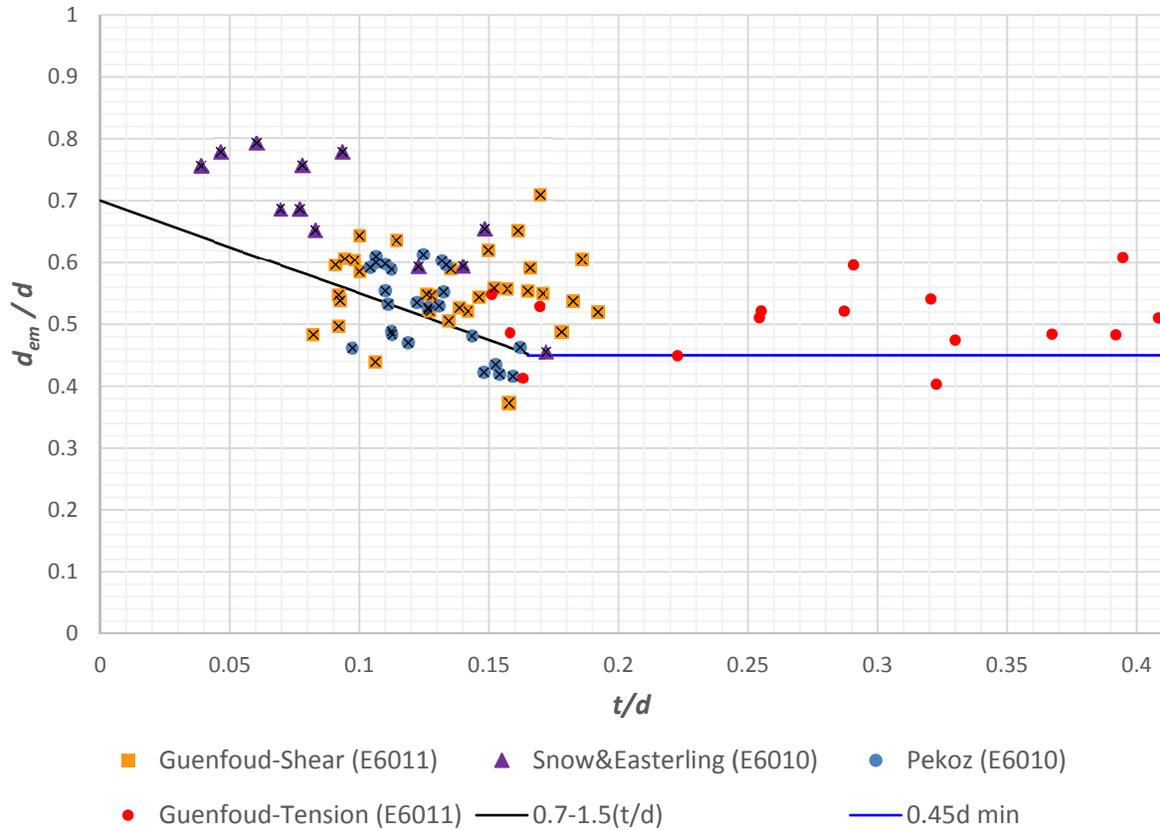
Figure 5.1: Proposed modification to effective weld diameter calculation.

Shear Tests

Overall, the increased data base improved the performance of the shear design equations. It's recommended that AISI consider raising the resistance and safety factors for E2.2.2.1-2 and E2.2.2.1-3 based on the analysis results shown in Tables 4-2 through 4-3. AISI S100-12 equation E2.2.2.1-4 did not apply to any other authors beyond Pekoz, therefore no change is recommended. For the shear weld strength calculation, AISI equation E2.2.2.1-1, this study recommends introducing a lower limit equal to 0.45d to AISI E2.2.2.1-5 as presented in Equation 4-1. This recommendation reduces underestimating the effective weld diameter of connections with thicker combined sheet thicknesses. This change maintains resistance and safety factors for

AISI equation E2.2.2.1-1 and significantly improves tension weld strength AISI equation E.2.2.3-1 discussed below.

Tension Tests

Tension weld fracture proved to be a rare failure mode when not using weld washers. The only author able to produce tension weld failure without the use of weld washers or poor quality welds was Guenfoud, which he did by welding through thicker combined sheet thicknesses up to 0.23 inches (5.84mm) thick. Analyzing Guenfoud's 16 tension weld failure samples, the combined use of AISI S100-12 equations E2.2.2.1-5 and E2.2.3-1 proved to be poor predictors of weld strength. This study recommends changing E2.2.2.1-5 to Equation 4-1 by adding the lower limit as well as introducing a reduction factor, "r" equal to 0.50 to E2.2.3-1 as shown below in Equation 5-1 for when weld washers are not used.

$$P_n = (r)\frac{\pi d_e^2}{4}F_{xx} \qquad \text{where r =0.50} \qquad \qquad \text{(Eq. 5-1)}$$

Equation 5-1 would represent tension weld strength in absence of a weld washer and would be accompanied by similar resistance and safety factors as presented in Table 4-5 and Table 4-6. It appears from Peuler and LaBoube's reports that weld washers help aid uniform stress distribution. Guenfoud recommends that in lieu of a 50% reduction, weld washers could be used to aid uniform stress distribution on the weld area. Also, when welding through thicker combined sheet thicknesses where weld fracture may be a concern, authors LaBoube, Peuler, and Guenfoud concurred that E6011 electrodes have the best penetrating power.

Strength of sheet tearing failure under tensile loading governed by Equation 1-8 (AISI S100-12 E2.2.3-2) was evaluated under interior, side-lap, and eccentric test configurations. Some distinctions were necessary in the strength calculations for each configuration. The interior sheet configuration performed well with Equation 1-8 as it is currently written and with the increased

data for analysis the resistance and safety factors should be increases as presented in Table 4-7 and Table 4-8. Arc spot welds that are eccentrically loaded in tension performed well under the current specified 50% reduction of the strength predicted by Equation 1-8, this study recommends a slight increase in the resistance and safety factors as reported in Table 4-9 and Table 4-10.

Analysis of LaBoube's and Guenfoud's work on side-lap configurations, it is clear that the design thickness needs to be equal to the thickness of the uppermost sheet, as this is where sheet failure occurred for all side-lap samples. By taking the design thickness as the thickness of the uppermost sheet, the need for a 30% reduction as currently specified in AISI S100-12 is no longer necessary.

Sheet Thickness Limitation

The expanded data base includes samples with combined sheet thicknesses up to 0.23 inches (5.84 mm), well over the AISI S100-12 maximum limit of 0.15 inches (3.81 mm). Based on analysis of both tension and shear data, it is clear that arc spot welds made through specimens in excess of 0.15 inches still achieved proper weld penetration. Specimens with combined sheet thicknesses up to 0.23 inches were included in all of the data analysis throughout this report. Including thicker specimens did not drive down performance of AISI S100-12 strength equations as demonstrated in Table 4-19. It is recommended that AISI increase the maximum combined sheet thickness from 0.15 inches to 0.25 inches for all arc spot weld configurations.

Future Research

It was apparent in the side-lap arc spot weld data that the four sheet configuration outperformed the two sheet configurations; Guenfoud observed that the increased sheet

resistance resulted in less deformation therefore reducing peeling of the sheets. Considering this in addition to LaBoube's weld washer work, it's likely the use of weld washers could enhance performance of side-lap connections by provided a more concentric stress distribution. To improve the strength predicted for side-lap arc spot welds, specifying weld washers would improve the resistance and safety factors.

Tension weld failure specimens governed by AISI S100-12 equation E2.2.3-1 were the most uncommon and worst performing data within the scope of this study. If AISI were to desire more arc spot research, tension weld failure strength predictions would benefit. It is clear that weld washers aid this connection type and make the 50% reduction to E2.2.3-1 unnecessary but still the number of specimens, coefficient of variation, and consequently the resistance and safety factors are poor for this data set and the performance of E2.2.3-1 has room for improvement.

It should be noted that cyclic loading and diaphragm performance has been performed on arc spot welds, but these effects were not analyzed in this study.

Below summarizes the changes to AISI S100-12 that this study recommends.

Summary of Recommended Changes

Combined Sheet Thickness Maximum (E2.2):

"Arc spot welds shall not be made on steel where the thinnest sheet exceeds **0.25 in** (0.15 in) in thickness, nor through a combination of steel sheets having a total thickness over **0.25 in** (0.15 in)".

Shear:

E2.2.2.1-1

E2.2.2.1-2

E2.2.2.1-3

E2.2.2.1-4

> No changes recommended to shear equations.

E2.2.2.1-5 d_e = the greater of $0.7d - 1.5t$

$0.45d$

> Remove the upper limit of 0.55d and add a lower limit of 0.45d to the d_e

Table 5-1: Recommendation for AISI Arc Spot Weld Shear Specifications

Limit State	Equation	d_a/t	ϕ (LRFD)	Ω (ASD)	ϕ (LSD)
Arc Spot Weld – Shear *(Current S100-12 Italicized)*					
Sheet Tearing	E2.2.2-2	$d_a/t \leq 0.815 \sqrt{(E/F_u)}$	0.80 *(0.70)*	1.95 *(2.20)*	0.65 *(0.60)*
Sheet Tearing	E2.2.2-3	$0.815 \sqrt{(E/F_u)} < d_a/t < 1.397 \sqrt{(E/Fu)}$	0.85 *(0.55)*	1.75 *(2.80)*	0.70 *(0.45)*
Sheet Tearing	E2.2.2-4	$1.397 \sqrt{(E/F_u)} \leq d_a/t$	0.45 *(0.50)*	3.30 *(3.05)*	0.35 *(0.40)*
Weld Fracture	E2.2.2-1	All	0.60 *(0.60)*	2.60 *(2.55)*	0.50 *(0.50)*

REVISED MAY 2018 (1) E2.2.2-4, Ω corrected from 3.25 to 3.30
REVISED MAY 2018 (1) E2.2.2-1, Ω corrected from 2.45 to 2.60

Tension:

E2.2.3-1 $\qquad P_n = (\underline{\mathbf{r}}) \dfrac{\pi d_e^2}{4} F_{xx}$

E2.2.3-2 $\qquad P_n = (\underline{\mathbf{r}}) \, 0.8 (F_u/F_y)^2 t d_a F_u$

> Add a reduction coefficient, "r" to both tension equations. See instructions on what value to input for "r" in the table

Table 5-2: Recommendation for AISI Arc Spot Weld Tension Specifications

Arc Spot Weld – Tension *(Current S100-12 Italicized)*										
					Panel and Deck			**Other**		
Limit State	**Equation**	**Sheet Configuration**	**Design Thickness - t**	**Reduction Factor - r**	ϕ **(LRFD)**	Ω **(ASD)**	ϕ **(LSD)**	ϕ **(LRFD)**	Ω **(ASD)**	ϕ **(LSD)**
Sheet Tearing	E2.2.3-2	Single or Multiple Sheet	Total sheet(s) thickness	1.0	0.75 *(0.60)*	2.00 *(2.50)*	0.60 *(0.50)*	0.65 *(0.50)*	2.35 *(3.00)*	0.50 *(0.40)*
		Side-lap	Thickness of uppermost sheet *(100%)*	1.0 *(0.7)*	0.55 *(0.60)*	2.90 *(2.50)*	0.40 *(0.50)*	0.45 *(0.50)*	3.50 *(3.00)*	0.35 *(0.40)*
		Edge (Eccentric Loading)	Total sheet(s) thickness	0.5 / w/washers 1.0	0.65 *(0.60)*	2.30 *(2.50)*	0.50 *(0.50)*	0.55 *(0.50)*	2.75 *(3.00)*	0.45 *(0.40)*
Weld Fracture	E2.2.3-1	All	Total sheet(s) thickness	0.5 *(1.0)* / w/washers 1.0	0.50 *(0.60)*	3.05 *(2.50)*	0.35 *(0.50)*	0.40 *(0.50)*	3.90 *(3.00)*	0.30 *(0.40)*

REVISED MAY 2018 E2.2.3-2, Design sheet thickness for sidelap condition corrected.
REVISED MAY 2018 E2.2.3-1, LSD ϕ for Panel and Deck corrected from 0.40 to 0.35.

REFERENCES

1. Albrecht, R. E. (1988). "Developments and Future Needs in Welding Cold-Formed Steel," Ninth International Specialty Conference on Cold-Formed Steel Structures, University of Missouri-Rolla, Rolla, MO.

2. American Iron and Steel Institute (1989). "Specification for the Design of Cold-Formed Steel Structural Members," 1986 Edition with 1989 Addendum, Washington D.C.

3. American Iron and Steel Institute (2012). "North American Specifications for the Design of Cold-Formed Steel Structural Members," AISI S100-12.

4. American Welding Society (1977). "Specification for Welding Sheet Steel in Structures," AWS D1.3-77, Miami, FL.

5. Blodgett, O. W. (1990). Committee Correspondence, Lincoln Electric Company, Cleveland, OH.

6. Church, K., Bogh, B. (2016). "Reevaluation of AISI Effective Diameter Equations for Arc Spot Welds," Unpublished Report for Verco Decking- A Nucor Company, Fontana, CA.

7. Dhalla, A. K., Pekoz, T. (1971). "Tests on Puddle and Fillet Weld Connections," Department of Structural Engineering, Cornell University, Ithaca, NY.

8. Easterling, S. E., Snow, G. L. (2008). "Strength of Arc Spot Welds Made in Single and Multiple Steel Sheets," Virginia Polytech Institute and State University, Blacksburg, VA.

9. Fraczek, J., Pekoz, T. (1975). "Tests on Puddle Weld Connections" (An Unpublished Letter Report) Department of Structural Engineering, Cornell University, Ithaca, NY.

10. Fung, C. (1978). "Strength of Arc-Spot Weld in Sheet Steel Construction," Project No. 175, Canadian Steel Industry Construction Council, North York, ON, Canada.

11. Guenfoud, N., Tremblay, R., Rodgers, C.A. (2010). "Experimental Program on the Shear Capacity and Tension Capacity of Arc-Spot Weld Connections for Multi-Overlap Roof Deck Panels," Research Report No. ST10-01, Department of Civil, Geological and Mining Engineering, Ecole Polytechnique, Montreal, QC, Canada.

12. LaBoube, R. A., Yu, W. (1991). "Tensile Strength of Welded Connections," Center for Cold-Formed Steel Structures Library. Paper 190. Missouri University of Science and Technology, Rolla, MO.

13. Pekoz, T., McGuire, W. (1979). "Welding of Sheet Steel," Research Report No. SG 79-2, American Iron and Steel Institute, Washington, D.C., US.

14. Peuler, M., Rodgers, C.A., Tremblay, R. (2002). "Inelastic Response of Arc-Spot Welded Deck-To-Frame Connections for Steel Roof Deck Diaphragms," Master's Thesis, Department of Civil Engineering and Applied Mechanics, McGill University, Montreal, Canada.

15. Yarnell, R.S. and Pekoz, T. (1973). "Tests on Field Welded Puddle and Fillet Weld Connections," Department of Structural Engineering, Cornell University, Ithaca, New York.

16. Yu, W. W. (1989). Committee Correspondence, University of Missouri-Rolla, Rolla, MO.

APPENDIX A
COMPREHENSIVE DATA ANALYSIS

Table A-1: Shear Weld Failure, Equation 1-1 (E2.2.2.1-1) Data

Specimen Name	No. of Plys	Design Thickness t (in)	Measured Visible Dia. d (in)	Equated d_e (in)	Lower Limit 0.45*d (in)	Control d_e (in)	F_{xx} (ksi)	Predicted Weld Resistance P_n (kips)	Measured Resistance P_t (kips)	P_t/P_n
Guenfoud 2010										
SM1641	4	0.1150	0.673	0.299	0.303	0.303	62	3.37	7.51	2.23
SM1642	4	0.1150	0.693	0.313	0.312	0.313	62	3.59	9.13	2.54
SM1643	4	0.1150	0.697	0.315	0.314	0.315	62	3.65	7.82	2.14
SM1644	4	0.1150	0.713	0.326	0.321	0.326	62	3.91	10.68	2.73
SM1841	4	0.0921	0.720	0.366	0.324	0.366	62	4.92	7.76	1.57
SM1842	4	0.0921	0.728	0.372	0.328	0.372	62	5.07	6.92	1.36
SM1843	4	0.0921	0.685	0.341	0.308	0.341	62	4.28	6.16	1.44
SM1844	4	0.0921	0.732	0.374	0.330	0.374	62	5.15	7.60	1.48
SM2043	4	0.0693	0.654	0.354	0.294	0.354	62	4.59	6.72	1.46
SM2243	4	0.0575	0.626	0.352	0.282	0.352	62	4.55	5.33	1.17
SM1621P	2	0.1150	0.768	0.365	0.345	0.365	62	4.89	9.96	2.04
SM1622P	2	0.1150	0.728	0.337	0.328	0.337	62	4.18	3.89	0.93
SM1623P	2	0.1150	0.677	0.302	0.305	0.305	62	3.41	10.68	3.13
SM1624P	2	0.1150	0.646	0.280	0.291	0.291	62	3.10	5.64	1.82
SM1821P	2	0.0921	0.665	0.328	0.299	0.328	62	3.94	3.84	0.98
SM1822P	2	0.0921	0.724	0.369	0.326	0.369	62	5.00	6.81	1.36
SM1823P	2	0.0921	0.650	0.317	0.292	0.317	62	3.68	5.58	1.51
SM1824P	2	0.0921	0.681	0.339	0.306	0.339	62	4.21	8.79	2.09
SM2021P	2	0.0693	0.693	0.381	0.312	0.381	62	5.34	8.25	1.55
SM2221P	2	0.0575	0.587	0.324	0.264	0.324	62	3.87	6.07	1.57
SM2224P	2	0.0575	0.701	0.404	0.315	0.404	62	6.01	6.07	1.01
SM1621T	2	0.0575	0.575	0.316	0.259	0.316	62	3.67	7.33	2.00
SM1622T	2	0.0575	0.634	0.357	0.285	0.357	62	4.69	7.91	1.69
SM1623T	2	0.0575	0.610	0.341	0.275	0.341	62	4.27	7.60	1.78
SM1641T	4	0.1150	0.598	0.246	0.269	0.269	62	2.66	5.73	2.15
SM1642T	4	0.1150	0.618	0.260	0.278	0.278	62	2.84	6.74	2.37
SM1643T	4	0.1150	0.630	0.269	0.283	0.283	62	2.95	6.05	2.05
SM1841T	4	0.0921	0.606	0.286	0.273	0.286	62	3.01	6.45	2.14
SM1842T	4	0.0921	0.587	0.272	0.264	0.272	62	2.73	5.85	2.14
SM1843T	4	0.0921	0.630	0.303	0.283	0.303	62	3.37	6.59	1.96
SM2043T	4	0.0693	0.606	0.320	0.273	0.320	62	3.77	7.04	1.86
SM2241T	4	0.0575	0.622	0.349	0.280	0.349	62	4.48	5.40	1.20
SM2243T	4	0.0575	0.626	0.352	0.282	0.352	62	4.55	6.02	1.32

Table A-2: Shear Weld Failure, Equation 1-1 (E2.2.2.1-1) Data Cont.

Specimen Name	No. of Plys	Design Thickness t (in)	Measured Visible Dia. d (in)	Equated d d_e (in)	Lower Limit 0.45*d (in)	Control d_e (in)	F_{xx} (ksi)	Predicted Weld Resistance P_n (kips)	Measured Resistance P_t (kips)	P_t/P_n
Pekoz 1979										
AA/B12/7D(B-C)1	1	0.101	0.90	0.48	0.41	0.48	60	8.09	10.30	1.27
AA/B12/7D(B-C)2	1	0.101	0.92	0.49	0.41	0.49	60	8.57	12.40	1.45
AA/B12/7D-C)3	1	0.102	0.92	0.49	0.41	0.49	60	8.52	10.15	1.19
AA/B12/7D(F-C)1	1	0.101	0.92	0.49	0.41	0.49	60	8.57	12.05	1.41
AA/B12/7D(F-C)2	1	0.101	0.95	0.51	0.43	0.51	60	9.32	12.45	1.34
AA/B12/7D(E-C)1	1	0.101	0.95	0.51	0.43	0.51	60	9.32	12.05	1.29
AA/B12/7D(E-C)2	1	0.102	0.98	0.53	0.44	0.53	60	10.04	12.05	1.20
AA/B12/7D(AA-C)1	1	0.101	1.04	0.58	0.47	0.58	60	11.75	12.25	1.04
AA/B12/7D(AA-C)3	1	0.101	0.90	0.48	0.41	0.48	60	8.09	7.00	0.87
AA/B 2/7C(E-AA)2	1	0.101	0.85	0.44	0.38	0.44	60	6.95	5.35	0.77
AA/B10/7D(E-CC)1	1	0.139	1.04	0.52	0.47	0.52	60	9.55	13.05	1.37
AA/B10/7D(E-CC)2	1	0.139	1.05	0.53	0.47	0.53	60	9.79	10.45	1.07
AA/B10/7D(E-E)1	1	0.139	1.14	0.59	0.51	0.59	60	12.27	17.25	1.41
AA/B10/7D(E-E)2	1	0.140	1.24	0.66	0.56	0.66	60	15.34	14.15	0.92
BA/B14/7D(A-C)1	2	0.154	1.01	0.48	0.45	0.48	60	8.01	8.60	1.07
BA/B14/7D(A-C)2	2	0.155	1.08	0.52	0.49	0.52	60	9.69	10.45	1.08
BA/B14/7D(D-C)1	2	0.154	1.04	0.50	0.47	0.50	60	8.73	8.05	0.92
BA/B14/7D(D-C)2	2	0.154	0.95	0.43	0.43	0.43	60	6.66	5.90	0.89
BA/B14/7D(F-C)1	2	0.154	1.00	0.47	0.45	0.47	60	7.77	7.40	0.95
BA/B14/7D(F-C)2	2	0.153	0.96	0.44	0.43	0.44	60	6.92	8.25	1.19
BA/B14/7D(D-E)1	2	0.153	1.16	0.58	0.52	0.58	60	11.99	19.45	1.62
BA/B14/7D(D-E)2	2	0.153	1.17	0.59	0.53	0.59	60	12.28	19.70	1.60
BA/B18/7C(D-AA)1	2	0.093	0.75	0.38	0.34	0.38	60	5.24	9.45	1.80
BA/B18/7C(D-AA)2	2	0.094	0.74	0.38	0.33	0.38	60	5.04	6.30	1.25
Fung 1978										
2AS-315	1	0.059	0.47	0.24	0.21	0.24	60	2.04	6.48	3.17
2AS-317	1	0.059	0.56	0.30	0.25	0.30	60	3.26	5.96	1.83
2AS-319	1	0.059	0.5	0.26	0.23	0.26	60	2.42	5.98	2.47
3BS-107	1	0.072	0.81	0.46	0.36	0.46	60	7.45	9.60	1.29
3BS-108	1	0.072	0.88	0.51	0.40	0.51	60	9.12	9.52	1.04
3BS-109	1	0.072	0.88	0.51	0.40	0.51	60	9.12	9.18	1.01
3BS-207	1	0.072	0.66	0.35	0.30	0.35	60	4.43	9.74	2.20
3BS-208	1	0.072	0.63	0.33	0.28	0.33	60	3.92	7.04	1.80
3BS-209	1	0.072	0.63	0.33	0.28	0.33	60	3.92	8.98	2.29
3BS-210	1	0.072	0.69	0.38	0.31	0.38	60	4.97	9.66	1.94
3BS-211	1	0.072	0.69	0.38	0.31	0.38	60	4.97	9.54	1.92
3BS-212	1	0.072	0.69	0.38	0.31	0.38	60	4.97	9.76	1.96

Table A-3: Shear Weld Failure, Equation 1-1 (E2.2.2.1-1) Data Cont.

Specimen Name	No. of Plys	Design Thickness t (in)	Measured Visible Dia. d (in)	Equated d_e (in)	Lower Limit 0.45*d (in)	Control d_e (in)	F_{xx} (ksi)	Predicted Weld Resistance P_n (kips)	Measured Resistance P_t (kips)	P_t/P_n
Snow 2009										
3/4, 20	2	0.068	0.833	0.481	0.375	0.481	60	8.18	6.78	0.83
3/4, 18, 1	2	0.092	0.721	0.367	0.324	0.367	60	4.75	8.13	1.71
3/4, 18, 2	2	0.092	0.801	0.423	0.360	0.423	60	6.31	9.84	1.56
3/4, 12, 3	2	0.092	0.804	0.425	0.362	0.425	60	6.38	7.92	1.24
3/4, 16, 1	2	0.114	0.800	0.389	0.360	0.389	60	5.35	5.62	1.05
3/4, 16, 2	2	0.114	0.760	0.361	0.342	0.361	60	4.61	6.38	1.39
3/4, 16, 3	2	0.114	0.749	0.353	0.337	0.353	60	4.41	8.12	1.84
3/4, 16, 4	2	0.114	0.757	0.359	0.341	0.359	60	4.55	3.77	0.83
5/8, 16, 1	1	0.057	0.639	0.362	0.288	0.362	60	4.63	6.12	1.32
5/8, 16, 2	1	0.057	0.679	0.390	0.306	0.390	60	5.37	6.71	1.25
5/8, 22	2	0.056	0.618	0.349	0.278	0.349	60	4.29	3.90	0.91
5/8, 20	2	0.068	0.602	0.319	0.271	0.319	60	3.61	6.45	1.79
5/8, 18, 1	2	0.092	0.620	0.296	0.279	0.296	60	3.10	4.39	1.42
5/8, 18, 2	2	0.092	0.635	0.307	0.286	0.307	60	3.32	6.24	1.88
5/8, 18, 3	2	0.092	0.692	0.346	0.311	0.346	60	4.24	3.50	0.83
5/8, 18, 4	2	0.092	0.729	0.372	0.328	0.372	60	4.90	3.40	0.69
5/8, 16, 1	2	0.114	0.658	0.290	0.296	0.296	60	3.10	3.91	1.26
5/8, 16, 2	2	0.114	0.658	0.290	0.296	0.296	60	3.10	5.55	1.79
5/8, 16, 3	2	0.114	0.639	0.276	0.288	0.288	60	2.92	4.70	1.61

Table A-4: Shear Sheet Failure, Equation 1-2 (E2.2.2.1-2) Data
Note that Peuler tested various weld electrodes, these are specified in column 1.

Specimen Name	No. of Plies	Design Thickness t (in)	Measured Visible Dia. d (in)	d_a (in)	d_a/t	Measured F_u (ksi)	$0.815*\sqrt{(E/F_u)}$	Predicted Sheet Resistance P_n (kips)	Measured Resistance P_t (kips)	P_t/P_n
Guenfoud 2010										
SM1621	2	0.0575	0.669	0.612	10.6	56.29	18.66	4.35	7.37	1.69
SM1622	2	0.0575	0.669	0.612	10.6	56.29	18.66	4.35	7.82	1.80
SM1623	2	0.0575	0.724	0.667	11.6	56.29	18.66	4.75	7.49	1.58
SM1624	2	0.0575	0.673	0.616	10.7	56.29	18.66	4.38	7.46	1.70
SM1821	2	0.0461	0.713	0.667	14.5	62.15	17.76	4.20	6.02	1.44
SM1822	2	0.0461	0.693	0.647	14.0	62.15	17.76	4.07	6.29	1.55
SM1823	2	0.0461	0.665	0.619	13.4	62.15	17.76	3.90	5.62	1.44
SM1824	2	0.0461	0.748	0.702	15.2	62.15	17.76	4.42	6.27	1.42
SM2021	2	0.0346	0.614	0.580	16.7	60.23	18.04	2.66	3.62	1.36
SM2022	2	0.0346	0.610	0.576	16.6	60.23	18.04	2.64	3.75	1.42
SM2023	2	0.0346	0.650	0.615	17.8	60.23	18.04	2.82	3.98	1.41
SM2024	4	0.0346	0.602	0.568	16.4	60.23	18.04	2.61	3.66	1.41
SM2041	4	0.0693	0.626	0.557	8.0	60.23	18.04	5.11	6.38	1.25
SM2042	4	0.0693	0.642	0.572	8.3	60.23	18.04	5.26	7.17	1.36
SM2044	4	0.0693	0.642	0.572	8.3	60.23	18.04	5.26	5.62	1.07
SM2241	4	0.0575	0.606	0.549	9.5	64.74	17.40	4.49	5.80	1.29
SM2242	4	0.0575	0.693	0.635	11.1	64.74	17.40	5.20	6.54	1.26
SM2022P	2	0.0693	0.744	0.675	9.7	60.23	18.04	6.20	7.24	1.17
SM2023P	2	0.0693	0.638	0.569	8.2	60.23	18.04	5.22	6.79	1.30
SM2024P	2	0.0693	0.701	0.631	9.1	60.23	18.04	5.80	6.61	1.14
SM2222P	2	0.0575	0.657	0.600	10.4	64.74	17.40	4.91	6.41	1.30
SM2223P	2	0.0575	0.638	0.580	10.1	64.74	17.40	4.75	6.07	1.28
SM1821T	2	0.0461	0.646	0.600	13.0	62.15	17.76	3.78	5.91	1.57
SM1822T	2	0.0461	0.504	0.458	9.9	62.15	17.76	2.88	4.63	1.61
SM1823T	2	0.0461	0.618	0.572	12.4	62.15	17.76	3.60	5.55	1.54
SM1824T	2	0.0461	0.567	0.521	11.3	62.15	17.76	3.28	4.79	1.46
SM2021T	2	0.0346	0.610	0.576	16.6	60.23	18.04	2.64	4.05	1.53
SM2022T	2	0.0346	0.642	0.607	17.5	60.23	18.04	2.79	4.11	1.48
SM2023T	2	0.0346	0.598	0.564	16.3	60.23	18.04	2.59	4.18	1.62
SM2041T	4	0.0693	0.606	0.537	7.8	60.23	18.04	4.93	6.14	1.24
SM2042T	4	0.0693	0.614	0.545	7.9	60.23	18.04	5.00	7.42	1.48
SM2044T	4	0.0693	0.618	0.549	7.9	60.23	18.04	5.04	6.99	1.39
SM2242T	4	0.0575	0.622	0.565	9.8	64.74	17.40	4.62	3.91	0.85
SM2244T	4	0.0575	0.594	0.537	9.3	64.74	17.40	4.40	6.02	1.37

Table A-4: Shear Sheet Failure, Equation 1-2 (E2.2.2.1-2) Data Cont.

Specimen Name (Electrode)	No. of Plies	Design Thickness t (in)	Measured Visible Dia. d (in)	d_a (in)	d_a/t	Measured F_u (ksi)	$0.815*\sqrt{(E/F_u)}$	Predicted Sheet Resistance P_n (kips)	Measured Resistance P_t (kips)	P_t/P_n
Peuler 2002										
13a E6010	1	0.059	0.80	0.74	12.64	54.56	18.95	5.22	8.29	1.59
13b	1	0.059	0.75	0.69	11.79	54.56	18.95	4.87	8.30	1.70
13c	1	0.059	0.75	0.69	11.79	54.56	18.95	4.87	8.54	1.75
13d	1	0.059	0.70	0.64	10.93	54.56	18.95	4.52	7.82	1.73
13e	1	0.059	0.73	0.67	11.44	54.56	18.95	4.73	8.51	1.80
16a	1	0.046	0.66	0.61	13.33	52.53	19.31	3.27	4.55	1.39
16b	1	0.046	0.61	0.56	12.24	52.53	19.31	3.00	5.42	1.81
16c	1	0.046	0.63	0.58	12.68	52.53	19.31	3.11	4.96	1.60
16d	1	0.046	0.59	0.54	11.81	52.53	19.31	2.90	5.17	1.78
16e	1	0.046	0.64	0.59	12.89	52.53	19.31	3.16	5.57	1.76
19a	1	0.035	0.56	0.52	14.80	59.13	18.20	2.42	2.03	0.84
19b	1	0.035	0.54	0.50	14.24	59.13	18.20	2.33	2.72	1.17
19c	1	0.035	0.54	0.50	14.24	59.13	18.20	2.33	2.84	1.22
19d	1	0.035	0.68	0.64	18.19	59.13	18.20	2.97	3.47	1.17
19e	1	0.035	0.65	0.61	17.34	59.13	18.20	2.83	3.82	1.35
59a	1	0.046	0.73	0.68	14.85	52.53	19.31	3.64	6.18	1.70
59b	1	0.046	0.70	0.65	14.20	52.53	19.31	3.48	5.04	1.45
59c	1	0.046	0.76	0.71	15.50	52.53	19.31	3.80	5.85	1.54
61a	1	0.046	0.53	0.48	10.51	52.53	19.31	2.58	2.52	0.98
61b	1	0.046	0.55	0.50	10.94	52.53	19.31	2.68	2.98	1.11
61c	1	0.046	0.62	0.57	12.46	52.53	19.31	3.06	2.96	0.97
46a E6011	1	0.059	0.78	0.72	12.30	54.56	18.95	5.08	8.68	1.71
46b	1	0.059	0.79	0.73	12.47	54.56	18.95	5.15	8.52	1.65
46c	1	0.059	0.76	0.70	11.96	54.56	18.95	4.94	7.78	1.58
46d	1	0.059	0.74	0.68	11.61	54.56	18.95	4.80	8.82	1.84
46e	1	0.059	0.77	0.71	12.13	54.56	18.95	5.01	8.66	1.73
47a	1	0.046	0.66	0.61	13.33	52.53	19.31	3.27	6.13	1.88
47b	1	0.046	0.62	0.57	12.46	52.53	19.31	3.06	5.80	1.90
47c	1	0.046	0.61	0.56	12.24	52.53	19.31	3.00	6.23	2.07
47d	1	0.046	0.64	0.59	12.89	52.53	19.31	3.16	5.79	1.83
47e	1	0.046	0.69	0.64	13.98	52.53	19.31	3.43	5.93	1.73
49a	1	0.029	0.41	0.38	13.07	55.69	18.76	1.36	2.24	1.65
49b	1	0.029	0.50	0.47	16.16	55.69	18.76	1.68	1.45	0.86
49c	1	0.029	0.53	0.50	17.19	55.69	18.76	1.79	2.38	1.33
49d	1	0.029	0.49	0.46	15.82	55.69	18.76	1.65	1.69	1.03
49e	1	0.029	0.48	0.45	15.48	55.69	18.76	1.61	1.23	0.76

Table A-4: Shear Sheet Failure, Equation 1-2 (E2.2.2.1-2) Data Cont.

Specimen Name (Electrode)	No. of Plys	Design Thickness t (in)	Measured Visible Dia. d (in)	d_a (in)	d_a/t	Measured F_u (ksi)	0.815* $\sqrt{(E/F_u)}$	Predicted Sheet Resistance P_n (kips)	Measured Resistance P_t (kips)	P_t/P_n
Peuler 2002 cont.										
71a-E6022	1	0.046	0.65	0.60	13.11	52.5	19.3	3.22	5.55	1.73
71b	1	0.046	0.50	0.45	9.85	52.5	19.3	2.42	4.21	1.74
71c	1	0.046	0.65	0.60	13.11	52.5	19.3	3.22	4.95	1.54
73a	1	0.029	0.55	0.52	17.88	55.7	18.8	1.86	2.56	1.37
73b	1	0.029	0.55	0.52	17.88	55.7	18.8	1.86	2.34	1.26
79a-E7018	1	0.046	0.68	0.63	13.76	52.5	19.3	3.37	5.11	1.51
79b	1	0.046	0.67	0.62	13.55	52.5	19.3	3.32	5.33	1.60
79c	1	0.046	0.66	0.61	13.33	52.5	19.3	3.27	4.49	1.37
Pekoz 1979										
AA/B18/7D1	1	0.049	0.79	0.74	15.12	64.4	17.4	5.14	6.74	1.31
AA/B18/7D2	1	0.050	0.80	0.75	15.00	64.4	17.4	5.31	6.2	1.17
AA/B18/7D3	1	0.049	0.81	0.76	15.53	64.4	17.4	5.28	6.55	1.24
AA/B18/7D4	1	0.050	0.85	0.80	16.00	64.4	17.4	5.67	7.2	1.27
Snow 2009										
3/4, 18, 1	1	0.046	0.742	0.696	15.13	55.3	18.82	3.90	4.65	1.19
3/4, 18, 2	1	0.046	0.700	0.654	14.22	55.3	18.82	3.66	4.78	1.31
3/4, 18, 3	1	0.046	0.726	0.680	14.78	55.3	18.82	3.81	4.74	1.25
3/4, 16, 1	1	0.057	0.746	0.689	12.09	61.2	17.89	5.29	6.53	1.23
3/4, 16, 2	1	0.057	0.773	0.716	12.56	61.2	17.89	5.49	6.97	1.27
3/4, 16, 3	1	0.057	0.732	0.675	11.84	61.2	17.89	5.18	6.78	1.31
3/4, 22, 1	2	0.056	0.826	0.770	13.75	55.3	18.82	5.25	5.36	1.02
3/4, 22, 2	2	0.056	0.730	0.674	12.04	55.3	18.82	4.59	5.48	1.19
3/4, 22, 3	2	0.056	0.765	0.709	12.66	55.3	18.82	4.83	5.64	1.17
3/4, 20, 1	2	0.068	0.760	0.692	10.18	58.7	18.27	6.08	7.41	1.22
3/4, 20, 2	2	0.068	0.775	0.707	10.40	58.7	18.27	6.21	7.40	1.19
3/4, 18	2	0.092	0.785	0.693	7.53	55.3	18.82	7.76	9.80	1.26
5/8, 20	1	0.034	0.608	0.574	16.88	58.7	18.27	2.52	3.38	1.34
5/8, 18, 1	1	0.046	0.685	0.639	13.89	55.3	18.82	3.58	4.71	1.32
5/8, 18, 2	1	0.046	0.690	0.644	14.00	55.3	18.82	3.60	4.58	1.27
5/8, 18, 3	1	0.046	0.617	0.571	12.41	55.3	18.82	3.20	4.46	1.40
5/8, 16	1	0.057	0.675	0.618	10.84	61.2	17.89	4.74	6.60	1.39
5/8, 22, 1	2	0.056	0.661	0.605	10.80	55.3	18.82	4.12	5.50	1.33
5/8, 22, 2	2	0.056	0.596	0.540	9.64	55.3	18.82	3.68	4.63	1.26
5/8, 22, 3	2	0.056	0.592	0.536	9.57	55.3	18.82	3.65	4.60	1.26
5/8, 20, 1	2	0.068	0.62	0.55	8.13	58.7	18.27	4.86	6.78	1.40
5/8, 20, 2	2	0.068	0.67	0.60	8.88	58.7	18.27	5.30	7.04	1.33

Table A-5: Shear Sheet Failure, Equation 1-3 (E2.2.2.1-3) Data

Specimen Name (Electrode)	No. of Plys	Design Thickness t (in)	Measured Visible Dia. d (in)	d_a (in)	d_a/t	Measured F_u (ksi)	0.815* √(E/Fu)	1.397* √(E/Fu)	Predicted Sheet Resistance P_n (kips)	Measured Resistance P_t (kips)	P_t/P_n
Guenfoud 2010											
SM2221	2	0.0287	0.630	0.601	20.9	64.74	17.40	29.82	2.10	3.15	1.50
SM2222	2	0.0287	0.669	0.641	22.3	64.74	17.40	29.82	2.12	3.44	1.62
SM2223	2	0.0287	0.681	0.652	22.7	64.74	17.40	29.82	2.13	3.33	1.56
SM2224	2	0.0287	0.654	0.625	21.7	64.74	17.40	29.82	2.11	3.44	1.63
SM2221T	2	0.0287	0.626	0.597	20.8	64.74	17.40	29.82	2.10	3.39	1.62
SM2222T	2	0.0287	0.583	0.554	19.3	64.74	17.40	29.82	2.08	3.15	1.52
SM2223T	2	0.0287	0.571	0.542	18.9	64.74	17.40	29.82	2.07	3.06	1.48
SM2224T	2	0.0287	0.602	0.574	20.0	64.74	17.40	29.82	2.09	3.42	1.64
Peuler 2002											
21a E6010	1	0.029	0.62	0.59	20.28	55.69	18.76	32.15	1.97	2.22	1.12
21b	1	0.029	0.66	0.63	21.65	55.69	18.76	32.15	1.99	3.45	1.74
21e	1	0.029	0.62	0.59	20.28	55.69	18.76	32.15	1.97	2.35	1.19
73c E6022	1	0.029	0.59	0.56	19.25	55.69	18.76	32.15	1.96	2.57	1.31
Snow and Easterling 2002											
3/4, 22, 1	1	0.028	0.703	0.675	24.1	55.3	18.82	32.27	1.86	2.50	1.34
3/4, 22, 2	1	0.028	0.720	0.692	24.7	55.3	18.82	32.27	1.87	2.45	1.31
3/4, 22, 3	1	0.028	0.730	0.702	25.1	55.3	18.82	32.27	1.87	2.73	1.46
3/4, 20, 1	1	0.034	0.722	0.688	20.2	58.7	18.27	31.32	2.77	3.43	1.24
3/4, 20, 2	1	0.034	0.702	0.668	19.6	58.7	18.27	31.32	2.75	3.39	1.23
3/4, 20, 3	1	0.034	0.801	0.767	22.6	58.7	18.27	31.32	2.81	3.62	1.29
5/8, 22, 1	1	0.028	0.602	0.574	20.5	55.3	18.82	32.27	1.82	2.27	1.25
5/8, 22, 2	1	0.028	0.670	0.642	22.9	55.3	18.82	32.27	1.85	2.42	1.31
5/8, 22, 3	1	0.028	0.631	0.603	21.5	55.3	18.82	32.27	1.83	2.51	1.37
5/8, 20, 1	1	0.034	0.680	0.646	19.0	58.7	18.27	31.32	2.74	3.59	1.31
5/8, 20, 2	1	0.034	0.665	0.631	18.6	58.7	18.27	31.32	2.73	3.36	1.23

Table A-6: Shear Sheet Failure, Equation 1-4 (E2.2.2.1-4) Data

Specimen Name (Electrode)	No. of Plies	Design Thickness t (in)	Measured Visible Dia. d (in)	d_a (in)	d_a/t	Measured F_u (ksi)	$1.397*\sqrt{(E/F_u)}$	Predicted Sheet Resistance P_n (kips)	Measured Resistance P_t (kips)	P_t/P_n
Pekoz 1979										
A A/B 28/7 C1	1	0.016	0.64	0.62	39.00	97.60	23.82	1.36	1.38	1.01
A E/B 28/7 C2	1	0.016	0.64	0.62	39.00	97.60	23.82	1.36	0.97	0.71
A E/B 28/7 C3	1	0.016	0.57	0.55	34.63	97.60	23.82	1.21	1.30	1.07
A E/B 28/7 C4	1	0.016	0.59	0.57	35.88	97.60	23.82	1.25	1.27	1.01
A E/B 28/7 C5	1	0.016	0.56	0.54	34.00	97.60	23.82	1.19	1.36	1.14

Table A-7: Tension Weld Failure, Equation 1-7 (E2.2.3-1) Data
(Created with the greater of 0.45d and $d_e = 0.7d-1.5t$ and a reduction factor = 0.50)

Specimen Name	No. of Plies	Design Thickness t (in)	Measured Visible Dia. d (in)	Equated d_e (in)	Lower Limit 0.45*d (in)	Control d_e (in)	F_{xx} (ksi)	Predicted Weld Resistance P_n (kips)	Measured Resistance P_t (kips)	P_t/P_n
Guenfoud 2010										
T1623	2	0.115	0.705	0.321	0.317	0.321	62.36	2.52	2.63	1.04
T1641	4	0.230	0.713	0.154	0.321	0.321	62.36	2.52	2.88	1.14
T1642	4	0.230	0.697	0.143	0.314	0.314	62.36	2.41	3.46	1.44
T1643	4	0.230	0.583	0.063	0.262	0.262	62.36	1.68	4.36	2.59
T1841	4	0.184	0.724	0.231	0.326	0.326	62.36	2.60	2.18	0.84
T2043	4	0.139	0.622	0.228	0.280	0.280	62.36	1.92	1.82	0.95
T1641T	4	0.230	0.587	0.066	0.264	0.264	62.36	1.71	2.09	1.23
T1642T	4	0.230	0.626	0.093	0.282	0.282	62.36	1.94	2.43	1.25
T1643T	4	0.230	0.563	0.049	0.253	0.253	62.36	1.57	2.07	1.32
T1821T	2	0.092	0.543	0.242	0.244	0.244	62.36	1.46	1.26	0.86
T1822T	2	0.092	0.583	0.270	0.262	0.270	62.36	1.78	1.21	0.68
T1823T	2	0.092	0.610	0.289	0.275	0.289	62.36	2.05	1.87	0.91
T1841T	4	0.184	0.634	0.167	0.285	0.285	62.36	1.99	2.92	1.47
T1842T	4	0.184	0.642	0.173	0.289	0.289	62.36	2.04	2.25	1.10
T1843T	4	0.184	0.575	0.126	0.259	0.259	62.36	1.64	2.79	1.70
T2041T	4	0.139	0.543	0.172	0.244	0.244	62.36	1.46	1.89	1.29

Table A-8: Tension Sheet Failure of Interior Configurations, Equation 1-8 (E2.2.3-2) Data

Note LaBoube's data included stick vs automated welds and are indicated in column 1. In addition, wider sheets were tested, where the width of the bottom of the corrugation was 3.375 inches (85.725 mm). These samples are also indicated in column 1.

Specimen Name	No. of Plies	Design Thickness t (in)	Measured Visible Dia. d (in)	d_a (in)	Measured F_u (ksi)	Measured F_y (ksi)	Predicted Sheet Resistance P_n (kips)	Measured Resistance P_t (kips)	P_t/P_n
Guenfoud 2010									
T1611	1	0.0575	0.598	0.541	56.29	51.69	1.66	1.71	1.03
T1612	1	0.0575	0.614	0.557	56.29	51.69	1.71	2.02	1.18
T1613	1	0.0575	0.539	0.482	56.29	51.69	1.48	1.57	1.06
T1614	1	0.0575	0.606	0.549	56.29	51.69	1.68	2.18	1.29
T1811	1	0.0461	0.610	0.564	62.15	51.88	1.85	1.93	1.04
T1812	1	0.0461	0.594	0.548	62.15	51.88	1.80	1.28	0.71
T1813	1	0.0461	0.594	0.548	62.15	51.88	1.80	1.71	0.95
T1814	1	0.0461	0.583	0.537	62.15	51.88	1.76	0.99	0.56
T2011	1	0.0346	0.555	0.520	60.23	50.13	1.25	1.57	1.25
T2012	1	0.0346	0.630	0.595	60.23	50.13	1.44	1.51	1.05
T2013	1	0.0346	0.681	0.646	60.23	50.13	1.56	1.42	0.91
T2014	1	0.0346	0.587	0.552	60.23	50.13	1.33	1.37	1.03
T2211	1	0.0287	0.567	0.538	64.74	56.83	1.04	0.90	0.86
T2212	1	0.0287	0.587	0.558	64.74	56.83	1.08	1.03	0.96
T2213	1	0.0287	0.535	0.507	64.74	56.83	0.98	0.92	0.94
LaBoube 1991									
GC1-Stick	1	0.029	0.45	0.425	47.99	39.12	0.71	0.96	1.34
GC2	1	0.029	0.48	0.451	47.99	39.12	0.76	0.86	1.14
GC3	1	0.029	0.487	0.458	47.99	39.12	0.77	1.12	1.46
GC4	1	0.029	0.558	0.529	47.99	39.12	0.89	1.15	1.30

Table A-8: Tension Sheet Failure of Interior Configurations, Equation 1-8 (E2.2.3-2) Data Cont.

Specimen Name (Electrode)	No. of Plies	Design Thickness t (in)	Measured Visible Dia. d (in)	d_a (in)	Measured F_u (ksi)	Measured F_y (ksi)	Predicted Sheet Resistance P_n (kips)	Measured Resistance P_t (kips)	P_t/P_n
LaBoube 1991 continued									
GC5-Stick	1	0.029	0.444	0.415	47.99	39.12	0.70	0.93	1.34
GC6	1	0.029	0.812	0.783	47.99	39.12	1.31	1.23	0.94
GC7	1	0.029	0.502	0.473	47.99	39.12	0.79	0.83	1.04
GC8	1	0.029	0.543	0.514	47.99	39.12	0.86	1.02	1.19
GC9	1	0.029	0.63	0.601	47.99	39.12	1.01	1.85	1.83
GC10	1	0.029	0.724	0.695	47.99	39.12	1.16	0.14	0.12
GC11	1	0.029	0.447	0.418	47.99	39.12	0.70	1.23	1.75
GC12	1	0.029	0.566	0.537	47.99	39.12	0.90	1.40	1.55
GC13	1	0.029	0.824	0.795	47.99	39.12	1.33	1.90	1.42
GC18A-Auto	1	0.029	0.396	0.367	47.99	39.12	0.61	0.64	1.03
GC20A	1	0.029	0.541	0.512	47.99	39.12	0.86	1.42	1.65
GC26A	1	0.029	0.378	0.349	47.99	39.12	0.58	0.94	1.61
GC28A	1	0.029	0.552	0.523	47.99	39.12	0.88	1.37	1.56
GC30A	1	0.029	0.391	0.362	47.99	39.12	0.61	0.94	1.54
GC31A	1	0.029	0.582	0.553	47.99	39.12	0.93	1.09	1.17
GC32A	1	0.029	0.399	0.370	47.99	39.12	0.62	0.93	1.49
GC33A	1	0.029	0.56	0.531	47.99	39.12	0.89	0.75	0.84
GC34A	1	0.029	0.641	0.612	47.99	39.12	1.03	1.41	1.38
GC35A	1	0.029	0.754	0.725	47.99	39.12	1.21	1.18	0.97
GC36A	1	0.029	0.583	0.554	47.99	39.12	0.93	1.42	1.52
GC37A	1	0.029	0.674	0.645	47.99	39.12	1.08	1.71	1.58
GC38A	1	0.029	0.702	0.673	47.99	39.12	1.13	1.23	1.09
GC39A	1	0.029	0.693	0.664	47.99	39.12	1.11	1.20	1.08
GC40A	1	0.029	0.667	0.638	47.99	39.12	1.07	1.35	1.27
GC41A	1	0.029	0.71	0.681	47.99	39.12	1.14	1.34	1.17
GC42A	1	0.029	0.654	0.625	47.99	39.12	1.05	1.25	1.20
GC43A	1	0.029	0.584	0.555	47.99	39.12	0.93	1.27	1.36
GC44A	1	0.029	0.753	0.724	47.99	39.12	1.21	1.39	1.14
GC45A	1	0.029	0.701	0.672	47.99	39.12	1.13	1.29	1.15
GC47A	1	0.029	0.614	0.585	47.99	39.12	0.98	1.90	1.93
GE1-Stick	1	0.029	0.459	0.430	79.86	79.54	0.80	0.89	1.11
GE2	1	0.029	0.418	0.389	79.86	79.54	0.73	0.99	1.36
GE3	1	0.029	0.431	0.402	79.86	79.54	0.75	1.03	1.37
GE4	1	0.029	0.834	0.805	79.86	79.54	1.50	2.08	1.38
GE5	1	0.029	0.444	0.415	79.86	79.54	0.78	1.09	1.41
GE6	1	0.029	0.64	0.611	79.86	79.54	1.14	1.21	1.06
GE7	1	0.029	0.437	0.408	79.86	79.54	0.76	1.14	1.49
GE8	1	0.029	0.607	0.578	79.86	79.54	1.08	1.42	1.32

Table A-8: Tension Sheet Failure of Interior Configurations, Equation 1-8 (E2.2.3-2) Data Cont.

Specimen Name (Electrode)	No. of Plies	Design Thickness t (in)	Measured Visible Dia. d (in)	d_a (in)	Measured F_u (ksi)	Measured F_y (ksi)	Predicted Sheet Resistance P_n (kips)	Measured Resistance P_t (kips)	P_t/P_n
LaBoube 1991 continued									
GE9-Stick	1	0.029	0.614	0.585	79.86	79.54	1.09	1.49	1.36
GE10	1	0.029	0.8	0.771	79.86	79.54	1.44	2.08	1.44
GE11	1	0.029	0.411	0.382	79.86	79.54	0.71	1.22	1.71
GE12	1	0.029	0.563	0.534	79.86	79.54	1.00	1.72	1.72
GE13	1	0.029	0.818	0.789	79.86	79.54	1.47	1.97	1.34
GE14	1	0.029	0.577	0.548	79.86	79.54	1.02	1.81	1.77
GE25A-Auto	1	0.029	0.377	0.348	79.86	79.54	0.65	0.75	1.15
GE27A	1	0.029	0.57	0.541	79.86	79.54	1.01	1.65	1.63
GE29A	1	0.029	0.321	0.292	79.86	79.54	0.55	0.73	1.33
GE31A	1	0.029	0.559	0.530	79.86	79.54	0.99	1.32	1.33
GE33A	1	0.029	0.278	0.249	79.86	79.54	0.47	0.49	1.05
GE35A	1	0.029	0.545	0.516	79.86	79.54	0.96	0.90	0.93
GE37A	1	0.029	0.387	0.358	79.86	79.54	0.67	0.91	1.35
GE38A	1	0.029	0.563	0.534	79.86	79.54	1.00	1.62	1.63
GE39A	1	0.029	0.395	0.366	79.86	79.54	0.68	0.98	1.44
GE40A	1	0.029	0.666	0.637	79.86	79.54	1.19	1.59	1.33
GE41A	1	0.029	0.756	0.727	79.86	79.54	1.36	1.44	1.06
GE42A	1	0.029	0.652	0.623	79.86	79.54	1.16	1.45	1.24
GE43A	1	0.029	0.699	0.670	79.86	79.54	1.25	1.23	0.98
GE44A	1	0.029	0.703	0.674	79.86	79.54	1.26	1.60	1.27
GE45A	1	0.029	0.669	0.640	79.86	79.54	1.20	1.22	1.02
GE46A	1	0.029	0.674	0.645	79.86	79.54	1.20	1.61	1.33
GE47A	1	0.029	0.693	0.664	79.86	79.54	1.24	1.59	1.28
GE48A	1	0.029	0.650	0.621	79.86	79.54	1.16	1.56	1.34
GE49A	1	0.029	0.648	0.619	79.86	79.54	1.16	1.56	1.35
GE50A	1	0.029	0.714	0.685	79.86	79.54	1.28	1.39	1.09
GE51A	1	0.029	0.710	0.681	79.86	79.54	1.27	1.29	1.01
GE52A	1	0.029	0.593	0.564	79.86	79.54	1.05	1.36	1.29
GC320-Wide	1	0.029	0.51	0.481	47.99	39.12	0.81	1.05	1.30
GC321	1	0.029	0.523	0.494	47.99	39.12	0.83	0.93	1.12
GC322	1	0.029	0.634	0.605	47.99	39.12	1.01	1.18	1.16
GC323	1	0.029	0.631	0.602	47.99	39.12	1.01	1.63	1.61
GC324	1	0.029	0.752	0.723	47.99	39.12	1.21	1.70	1.40
GC325	1	0.029	0.744	0.715	47.99	39.12	1.20	1.93	1.61

Table A-8: Tension Sheet Failure of Interior Configurations, Equation 1-8 (E2.2.3-2) Data Cont.

Specimen Name	No. of Plies	Design Thickness t (in)	Measured Visible Dia. d (in)	d_a (in)	Measured F_u (ksi)	Measured F_y (ksi)	Predicted Sheet Resistance P_n (kips)	Measured Resistance P_t (kips)	P_t/P_n
LaBoube 1991 continued									
GE320	1	0.029	0.496	0.467	79.86	79.54	0.87	1.30	1.49
GE321	1	0.029	0.472	0.443	79.86	79.54	0.83	1.05	1.27
GE322	1	0.029	0.592	0.563	79.86	79.54	1.05	2.03	1.93
GE323	1	0.029	0.633	0.604	79.86	79.54	1.13	1.38	1.22
GE324	1	0.029	0.895	0.866	79.86	79.54	1.62	1.60	0.99
GE325	1	0.029	0.753	0.724	79.86	79.54	1.35	1.33	0.98
GX20	1	0.0625	0.633	0.571	45.02	36.36	1.97	2.10	1.07
GX21	1	0.0625	0.567	0.505	45.02	36.36	1.74	2.15	1.23
GX22	1	0.0625	0.798	0.736	45.02	36.36	2.54	1.98	0.78
GX23	1	0.0625	0.697	0.635	45.02	36.36	2.19	3.23	1.47
GX24	1	0.0625	0.942	0.88	45.02	36.36	3.04	4.05	1.33
GX25	1	0.0625	0.931	0.869	45.02	36.36	3.00	2.80	0.93
GC200D	2	0.058	0.531	0.473	47.99	39.12	1.59	1.90	1.20
GC201D	2	0.058	0.500	0.442	47.99	39.12	1.48	2.19	1.48
GC202D	2	0.058	0.719	0.661	47.99	39.12	2.22	4.08	1.84
GC203D	2	0.058	0.813	0.755	47.99	39.12	2.53	4.15	1.64
GC204D	2	0.058	0.640	0.582	47.99	39.12	1.95	2.66	1.36
GC205D	2	0.058	0.766	0.708	47.99	39.12	2.37	2.85	1.20
GC206D	2	0.058	0.680	0.622	47.99	39.12	2.08	3.75	1.80
GC207D	2	0.058	0.785	0.727	47.99	39.12	2.44	3.53	1.45
GC208D	2	0.058	0.885	0.827	47.99	39.12	2.77	3.75	1.35
GC209D	2	0.058	0.812	0.754	47.99	39.12	2.53	3.98	1.57
GC210D	2	0.058	0.779	0.721	47.99	39.12	2.42	3.38	1.40
GE200D	2	0.058	0.625	0.567	79.86	79.54	2.12	1.96	0.93
GE201D	2	0.058	0.524	0.466	79.86	79.54	1.74	2.56	1.47
GE202D	2	0.058	0.647	0.589	79.86	79.54	2.20	2.88	1.31
GE203D	2	0.058	0.698	0.640	79.86	79.54	2.39	2.80	1.17
GE204D	2	0.058	0.763	0.705	79.86	79.54	2.63	3.03	1.15
GE205D	2	0.058	0.718	0.660	79.86	79.54	2.47	2.88	1.17
GE206D	2	0.058	0.539	0.481	79.86	79.54	1.80	1.93	1.07

Table A-9: Tension Sheet Failure of Eccentric Samples, Equation 1-8 (E2.2.3-2) Data

Specimen Name	No. of Plies	Design Thickness t (in)	Measured Visible Dia. d (in)	d_a (in)	Measured F_u (ksi)	Measured F_y (ksi)	Predicted Sheet Resistance P_n (kips)	Measured Resistance P_t (kips)	P_t/P_n
LaBoube 1991									
GC100-Auto	1	0.0290	0.555	0.526	47.99	39.12	0.441	0.450	1.02
GC101	1	0.0290	0.538	0.509	47.99	39.12	0.426	0.520	1.22
GC103	1	0.0290	0.592	0.563	47.99	39.12	0.472	0.693	1.47
GC105	1	0.0290	0.354	0.325	47.99	39.12	0.272	0.450	1.65
GC106	1	0.0290	0.387	0.358	47.99	39.12	0.300	0.445	1.48
GC107	1	0.0290	0.563	0.534	47.99	39.12	0.447	0.838	1.87
GC108	1	0.0290	0.572	0.543	47.99	39.12	0.455	0.750	1.65
GC109	1	0.0290	0.625	0.596	47.99	39.12	0.499	0.830	1.66
GC110	1	0.0290	0.664	0.635	47.99	39.12	0.532	0.890	1.67
GC111	1	0.0290	0.760	0.731	47.99	39.12	0.612	0.600	0.98
GC112	1	0.0290	0.707	0.678	47.99	39.12	0.568	0.640	1.13
GC115-Stick	1	0.0290	0.470	0.441	47.99	39.12	0.369	0.600	1.62
GC116	1	0.0290	0.467	0.438	47.99	39.12	0.367	0.600	1.64
GC117	1	0.0290	0.626	0.597	47.99	39.12	0.500	0.665	1.33
GC118	1	0.0290	0.632	0.603	47.99	39.12	0.505	0.980	1.94
GC120	1	0.029	0.906	0.877	47.99	39.12	0.735	1.435	1.953
GE100-Auto	1	0.029	0.54	0.506	99.83	99.43	0.591	0.805	1.36
GE101	1	0.029	0.554	0.525	99.83	99.43	0.613	0.488	0.80
GE103	1	0.029	0.561	0.532	99.83	99.43	0.621	0.865	1.39
GE104	1	0.029	0.546	0.517	99.83	99.43	0.604	0.830	1.38
GE105	1	0.029	0.365	0.336	99.83	99.43	0.392	0.420	1.07
GE106	1	0.029	0.328	0.299	99.83	99.43	0.349	0.183	0.52
GE107	1	0.029	0.562	0.533	99.83	99.43	0.622	0.730	1.17
GE108	1	0.029	0.552	0.523	99.83	99.43	0.611	0.945	1.55
GE109	1	0.029	0.633	0.604	99.83	99.43	0.705	0.600	0.85
GE110	1	0.029	0.639	0.610	99.83	99.43	0.712	0.620	0.87
GE111	1	0.029	0.717	0.688	99.83	99.43	0.803	0.720	0.90
GE112	1	0.029	0.708	0.679	99.83	99.43	0.793	0.695	0.88
GE115-Stick	1	0.029	0.533	0.504	99.83	99.43	0.588	0.887	1.51
GE116	1	0.029	0.551	0.522	99.83	99.43	0.609	0.900	1.48
GE117	1	0.029	0.713	0.684	99.83	99.43	0.798	0.850	1.065
GE118	1	0.029	0.772	0.743	99.83	99.43	0.867	0.725	0.836
GE119	1	0.029	0.887	0.858	99.83	99.43	1.002	0.945	0.943
GE120	1	0.029	0.938	0.909	99.83	99.43	1.06	0.835	0.787

Table A-9: Tension Sheet Failure of Eccentric Samples, Equation 1-8 (E2.2.3-2) Data Cont.

Specimen Name	No. of Plies	Design Thickness t (in)	Measured Visible Dia. d (in)	d_a (in)	Measured F_u (ksi)	Measured F_y (ksi)	Predicted Sheet Resistance P_n (kips)	Measured Resistance P_t (kips)	P_t/P_n
LaBoube 1991 continued									
GXl-Wide	1	0.0625	0.647	0.585	45.02	36.36	1.01	0.95	0.94
GX2	1	0.0625	0.587	0.525	45.02	36.36	0.91	1.10	1.22
GX3	1	0.0625	0.684	0.622	45.02	36.36	1.07	1.55	1.45
GX4	1	0.0625	0.682	0.62	45.02	36.36	1.07	1.40	1.31
GX5	1	0.0625	1.091	1.029	45.02	36.36	1.77	2.03	1.14
GX6	1	0.0625	0.989	0.927	45.02	36.36	1.60	1.65	1.03

Table A-10: Tension Sheet Failure of Side-laps, Equation 1-8 (E2.2.3-2) Data.
(Shown with t = half of combined sheet thickness and a reduction factor = 0.70)

Specimen Name	No. of Plies	Design Thickness t (in)	Measured Visible Dia. d (in)	d_a (in)	Measured F_u (ksi)	Measured F_y (ksi)	Predicted Sheet Resistance P_n (kips)	Measured Resistance P_t (kips)	P_t/P_n
LaBoube 1991									
GCS4- Stick	2	0.0290	0.700	0.671	47.99	39.12	0.787	0.675	0.858
GEL6	2	0.0290	0.793	0.764	99.83	99.43	1.249	1.400	1.121
GELS	2	0.0290	0.786	0.757	99.83	99.43	1.237	1.100	0.889
GCL6	2	0.0290	0.739	0.710	47.99	39.12	0.833	1.450	1.741
GCL5	2	0.0290	0.668	0.639	47.99	39.12	0.749	1.075	1.434
GCL3	2	0.0290	0.642	0.613	47.99	39.12	0.719	1.800	2.504
GEL4	2	0.0290	0.621	0.592	99.83	99.43	0.968	1.050	1.085
GEL3	2	0.0290	0.613	0.584	99.83	99.43	0.954	1.800	1.886
GCL4	2	0.0290	0.590	0.561	47.99	39.12	0.658	0.975	1.482
GCS3	2	0.0290	0.713	0.684	47.99	39.12	0.802	1.075	1.340
GES3	2	0.0290	0.565	0.536	99.83	99.43	0.876	0.825	0.942
GEL2	2	0.0290	0.506	0.477	99.83	99.43	0.780	1.450	1.860
GELI	2	0.0290	0.505	0.476	99.83	99.43	0.778	1.075	1.382
GCL2	2	0.0290	0.496	0.467	47.99	39.12	0.548	0.925	1.689
Guenfoud 2010									
T1621	2	0.0575	0.622	0.565	56.29	51.69	1.21	2.90	2.39
T1622	2	0.0575	0.638	0.580	56.29	51.69	1.25	3.53	2.83
T1624	2	0.0575	0.681	0.624	56.29	51.69	1.34	2.74	2.05
T1821	2	0.0461	0.689	0.643	62.15	51.88	1.48	2.50	1.69
T1822	2	0.0461	0.693	0.647	62.15	51.88	1.49	2.32	1.56
T1823	2	0.0461	0.661	0.615	62.15	51.88	1.42	2.25	1.59
T1824	2	0.0461	0.728	0.682	62.15	51.88	1.57	2.29	1.46

Table A-10: Tension Sheet Failure of Side-laps, Equation 1-8 (E2.2.3-2) Data Cont.
(Shown with t = half of combined sheet thickness and a reduction factor = 0.70)

Specimen Name	No. of Plies	Design Thickness t (in)	Measured Visible Dia. d (in)	d_a (in)	Measured F_u (ksi)	Measured F_y (ksi)	Predicted Sheet Resistance P_n (kips)	Measured Resistance P_t (kips)	P_t/P_n
Guenfoud 2010 continued									
T2021	2	0.035	0.622	0.587	60.23	50.13	0.99	1.28	1.29
T2022	2	0.035	0.646	0.611	60.23	50.13	1.03	1.17	1.13
T2023	2	0.035	0.634	0.599	60.23	50.13	1.01	1.26	1.24
T2221	2	0.029	0.626	0.597	64.74	56.83	0.81	1.17	1.45
T2222	2	0.029	0.673	0.644	64.74	56.83	0.87	1.12	1.29
T2223	2	0.029	0.697	0.668	64.74	56.83	0.90	1.62	1.79
T2224	2	0.029	0.709	0.680	64.74	56.83	0.92	1.10	1.20
T1621T	2	0.057	0.555	0.498	56.29	51.69	1.07	2.14	2.00
T1622T	2	0.057	0.547	0.490	56.29	51.69	1.05	2.14	2.03
T1623T	2	0.057	0.614	0.557	56.29	51.69	1.20	1.96	1.64
T2021T	2	0.035	0.531	0.497	60.23	50.13	0.84	1.39	1.66
T2022T	2	0.035	0.626	0.591	60.23	50.13	1.00	1.39	1.40
T2023T	2	0.035	0.642	0.607	60.23	50.13	1.02	0.81	0.79
T2221T	2	0.029	0.622	0.593	64.74	56.83	0.80	0.88	1.09
T2222T	2	0.029	0.594	0.566	64.74	56.83	0.77	0.45	0.59
T2223T	2	0.029	0.630	0.601	64.74	56.83	0.81	0.99	1.22
T2224T	2	0.029	0.504	0.475	64.74	56.83	0.64	1.17	1.82
T2225T	2	0.029	0.543	0.515	64.74	56.83	0.70	1.08	1.55
T1842	4	0.092	0.638	0.546	62.15	51.88	2.51	3.71	1.48
T1843	4	0.092	0.693	0.601	62.15	51.88	2.76	3.42	1.24
T1844	4	0.092	0.665	0.573	62.15	51.88	2.64	3.39	1.29
T2041	4	0.069	0.689	0.620	60.23	50.13	2.09	2.97	1.42
T2042	4	0.069	0.701	0.631	60.23	50.13	2.13	2.92	1.37
T2044	4	0.069	0.681	0.612	60.23	50.13	2.06	2.86	1.38
T2241	4	0.057	0.638	0.580	64.74	56.83	1.57	2.16	1.37
T2242	4	0.057	0.654	0.596	64.74	56.83	1.61	2.07	1.28
T2243	4	0.057	0.642	0.584	64.74	56.83	1.58	1.87	1.18
T2042T	4	0.069	0.587	0.517	60.23	50.13	1.75	2.50	1.43
T2043T	4	0.069	0.571	0.502	60.23	50.13	1.69	2.20	1.30
T2241T	4	0.057	0.622	0.565	64.74	56.83	1.53	1.78	1.16
T2242T	4	0.057	0.634	0.576	64.74	56.83	1.56	1.71	1.10
T2243T	4	0.057	0.622	0.565	64.74	56.83	1.53	2.52	1.65
T2244T	4	0.057	0.543	0.486	64.74	56.83	1.31	1.35	1.03

APPENDIX B
CALCULATION OF RESISTANCE AND SAFETY FACTORS

E2.2.2.1-1 using the greater of: 0.45d and d_e

<u>Contributing Authors:</u>
Guenfoud 2010
Snow 2009
Pekoz 1979
Fung 1978

Design Factor Calculation (US)		
C_ϕ	1.52	for LRFD
M_m	1.1	for spot welds
F_m	1.0	for spot welds
P_m	1.53	P_u/P_n average
β_o	3.5	for connections in LRFD
V_M	0.1	for spot welds
V_F	0.1	for spot welds
n	87	No. of sample total
C_P	1.04	Correction factor
V_P	0.326	COV
V_Q	0.21	for spot welds
ϕ	**0.591**	(LRFD)
Ω	**2.587**	(ASD)

Design Factor Calculation (CAN)		
C_ϕ	1.42	for LSD
M_m	1.1	for spot welds
F_m	1.0	for spot welds
P_m	1.53	P_u/P_n average
β_o	4	for connections in LSD
V_M	0.1	for spot welds
V_F	0.1	for spot welds
n	87	No. of sample total
C_P	1.04	Correction factor
V_P	0.326	COV
V_Q	0.21	for spot welds
ϕ	**0.448**	(LSD)

E2.2.2.1-2

<u>Contributing Authors:</u>
Guenfoud 2010
Snow 2009
Peuler 2002
Pekoz 1979

Design Factor Calculation (US)		
C_ϕ	1.52	for LRFD
M_m	1.1	for spot welds
F_m	1.0	for spot welds
P_m	1.38	P_u/P_n average
β_o	3.5	for connections in LRFD
V_M	0.1	for spot welds
V_F	0.1	for spot welds
n	104	No. of sample total
C_P	1.030	Correction factor
V_P	0.182	COV
V_Q	0.21	for spot welds
ϕ	**0.787**	(LRFD)
SF	**1.943**	(ASD)

Design Factor Calculation (CAN)		
C_ϕ	1.42	for LSD
M_m	1.1	for spot welds
F_m	1.0	for spot welds
P_m	1.38	P_u/P_n average
β_o	4.0	for connections in LSD
V_M	0.1	for spot welds
V_F	0.1	for spot welds
n	104	No. of sample total
C_P	1.030	Correction factor
V_P	0.182	COV
V_Q	0.21	for spot welds
ϕ	**0.629**	(LSD)

E2.2.2.1-3

Contributing Authors:
Guenfoud 2010
Snow 2009
Peuler 2002

Design Factor Calculation (US)		
C_ϕ	1.52	for LRFD
M_m	1.1	for spot welds
F_m	1.0	for spot welds
P_m	1.403	P_u/P_n average
β_o	3.5	for connections in LRFD
V_M	0.1	for spot welds
V_F	0.1	for spot welds
n	23	No. of sample total
C_P	1.15	Correction factor
V_P	0.123	COV
V_Q	0.21	for spot welds
ϕ	**0.865**	(LRFD)
Ω	**1.770**	(ASD)

Design Factor Calculation (CAN)		
C_ϕ	1.42	for LSD
M_m	1.1	for spot welds
F_m	1.0	for spot welds
P_m	1.403	P_u/P_n average
β_o	4.0	for connections in LSD
V_M	0.1	for spot welds
V_F	0.1	for spot welds
n	23	No. of sample total
C_P	1.15	Correction factor
V_P	0.123	COV
V_Q	0.21	for spot welds
ϕ	**0.700**	(LSD)

E2.2.2.1-4

Contributing Authors:

Pekoz 1979

Design Factor Calculation (US)		
C_ϕ	1.52	for LRFD
M_m	1.1	for spot welds
F_m	1.0	for spot welds
P_m	0.990	P_u/P_n average
β_o	3.5	for connections in LRFD
V_M	0.1	for spot welds
V_F	0.1	for spot welds
n	5	No. of sample total
C_P	2.4	Correction factor
V_P	0.167	COV
V_Q	0.21	for spot welds
ϕ	**0.467**	(LRFD)
Ω	**3.279**	(ASD)

Design Factor Calculation (CAN)		
C_ϕ	1.42	for LSD
M_m	1.1	for spot welds
F_m	1.0	for spot welds
P_m	0.990	P_u/P_n average
β_o	4	for connections in LSD
V_M	0.1	for spot welds
V_F	0.1	for spot welds
n	5	No. of sample total
C_P	2.4	Correction factor
V_P	0.167	COV
V_Q	0.21	for spot welds
ϕ	**0.364**	(LSD)

E2.2.3-1 using 0.45d ≤ d_e and r =0.50

<u>Contributing Authors:</u>

Guenfoud 2010

Design Factor Calculation (US)		
C_ϕ	1.52	for LRFD
M_m	1.1	for spot welds
F_m	1.0	for spot welds
P_m	1.24	P_u/P_n average for connections in LRFD
β_o	3.0	
V_M	0.1	for spot welds
V_F	0.1	for spot welds
n	16	No. of sample total
C_P	1.23	Correction factor
V_P	0.362	COV
V_Q	0.21	for spot welds
ϕ	**0.499**	(LRFD)
Ω	**3.066**	(ASD)

Design Factor Calculation (CAN)		
C_ϕ	1.42	for LSD
M_m	1.1	for spot welds
F_m	1.0	for spot welds
P_m	1.24	P_u/P_n average for connections in LSD
β_o	4	
V_M	0.1	for spot welds
V_F	0.1	for spot welds
n	16	No. of sample total
C_P	1.23	Correction factor
V_P	0.362	COV
V_Q	0.21	for spot welds
ϕ	**0.368**	(LSD)

E2.2.3-2 Interior configruation

<u>Contributing Authors:</u>

Guenfoud 2010

LaBoube 1991

Design Factor Calculation (US)		
C_ϕ	1.52	for LRFD
M_m	1.1	for spot welds
F_m	1.0	for spot welds
P_m	1.27	P_u/P_n average for connections in LRFD
β_o	3.0	
V_M	0.1	for spot welds
V_F	0.1	for spot welds
n	121	No. of sample total
C_P	1.03	Correction factor
V_P	0.223	COV
V_Q	0.21	for spot welds
ϕ	**0.767**	(LRFD)
SF	**1.994**	(ASD)

Design Factor Calculation (CAN)		
C_ϕ	1.42	for LSD
M_m	1.1	for spot welds
F_m	1.0	for spot welds
P_m	1.27	P_u/P_n average
β_o	3.5	for connections in LSD
V_M	0.1	for spot welds
V_F	0.1	for spot welds
n	121	No. of sample total
C_P	1.025	Correction factor
V_P	0.223	COV
V_Q	0.21	for spot welds
ϕ	**0.605**	(LSD)

APPENDIX C
EXAMPLE CALCULATIONS

Each illustrates a weld limit state using first, the existing AISI equations and design factors and second, the proposed equations and design factors followed by a comparison of both calculations for each limit state in the summary.

1. SHEAR: FAILURE THROUGH THE WELD

   a. **E2.2.2.1-1**

   $$P_n = \frac{\pi d_e^2}{4} 0.75 F_{xx}$$

   Proposed Modification: d_e = the greater of $\left| \begin{array}{l} 0.7d - 1.5t \\ \\ 0.45d \end{array} \right.$

Design Factor	Existing	Recalibrated with S100-12 de equation	Proposed with modified d_e equation
ϕ (LRFD, β = 3.5)	0.60	0.591	0.60

   i. Example: Existing d_e equation and design factor with $t < 0.07$".

   $t = 0.03"$

   $d = 0.625"$

   $E = 29{,}500 \text{ ksi}$

   $F_{xx} = 60 \text{ ksi}$

   $d_e = 0.7d - 1.5t = 0.7(0.625") - 1.5(0.03") = 0.3925"$

   $d_e \text{ max} = 0.55(d) = 0.55(0.625") = 0.344" \text{ (max controls)}$

   $\phi P_n = \phi \frac{\pi d_e^2}{4} 0.75 F_{xx}, \phi = 0.60$

   $\phi P_n = (0.6) \frac{\pi (0.344")^2}{4} 0.75(60\text{ksi})$

   $\underline{\phi P_n = 2.509 \text{ kips}}$

ii.   Example: Proposed d_e equation and recalibrated design factor with $t < 0.07$".

    $t = 0.03$"

    Use $d_e = 0.7d - 1.5t$, with **$0.45d < d_e$**

    $d_e = 0.7d - 1.5t = 0.7(0.625") - 1.5(0.03") = 0.3925"$ (largest controls)

    d_e min $= 0.45(d) = 0.45(0.625") = 0.281"$

    $\phi P_n = \phi \frac{\pi d_e^2}{4} 0.75 F_{xx}, \phi = \mathbf{0.60}$

    $\phi P_n = (\mathbf{0.60}) \frac{\pi(0.3925")^2}{4} 0.75(60\text{ksi})$

    $\underline{\phi P_n = 3.27 \text{ kips}}$

iii.   Example: Existing d_e equation and design factor with $t > 0.07$".

    $t = 0.12"$
    $d = 0.625"$

    $E = 29{,}500$ ksi

    $F_{xx} = 60$ ksi

    $d_e = 0.7d - 1.5t = 0.7(0.625") - 1.5(0.12") = 0.258"$ (controls)

    d_e max $= 0.55(d) = 0.55(0.625") = 0.344"$

    $\phi P_n = \phi \frac{\pi d_e^2}{4} 0.75 F_{xx}, \phi = 0.60$

    $\phi P_n = (0.60) \frac{\pi(0.258")^2}{4} 0.75(60\text{ksi})$

    $\underline{\phi P_n = 1.412 \text{ kips}}$

iv.   Example: Proposed d_e equation and recalibrated design factor with $t > 0.07$".

    $t = 0.12$"

$d_e = 0.7d - 1.5t$, with $\mathbf{0.45d < d_e}$

$d_e = 0.7d - 1.5t = 0.7(0.625") - 1.5(0.12") = 0.258"$

$\mathbf{d_e\ min = 0.45(d) = 0.45(0.625") = 0.281"}$ **(largest controls)**

$\phi P_n = \phi\ \dfrac{\pi d_e{}^2}{4} 0.75 F_{xx}, \phi = \mathbf{0.60}$

$\phi P_n = (\mathbf{0.60})\ \dfrac{\pi(\mathbf{0.281"})^2}{4} 0.75(60\text{ksi})$

$\underline{\mathbf{\phi P_n = 1.68\ kips}}$

2. SHEAR: FAILURE THROUGH THE SHEET

  a. E2.2.2.1-2

For $d_a/t \leq 0.815\ \sqrt{(E/F_u)} : P_n = 2.20td_aF_u$

Design Factor	Existing	Recalibrated	Proposed
ϕ (LRFD) ($\beta = 3.5$)	0.70	0.787	0.80

    i. Example: Existing Design Factor.

    $t = 0.03"$

    $d_a = 0.465"$

    $E = 29{,}500$ ksi

    $F_y = 60$ ksi

    $d_a/t = 0.465"/0.03" = 15.52$

    $0.815\ \sqrt{\dfrac{E}{F_u}} = 0.815\ \sqrt{29{,}500\ \text{ksi}/60\ \text{ksi}} = 18.07$

$$d_a/t = 15.52 < 0.815\sqrt{\frac{E}{F_u}} = 18.07 \qquad \text{Therefore E2.2.1.2 applies}$$

$$\phi P_n = \phi 2.20 t d_a F_u; \quad \phi = 0.70$$

$$\phi P_n = (0.70)2.20(0.003")(0.465")(60 \text{ ksi})$$

$$\underline{\phi P_n = 0.129 \text{ kips}}$$

ii.   Example: Recalibrated Design Factor.

$$d_a/t = {0.465"}/{0.03"} = 15.52$$

$$0.815\sqrt{\frac{E}{F_u}} = 0.815\sqrt{{29,500 \text{ ksi}}/{60 \text{ ksi}}} = 18.07$$

$$d_a/t = 15.52 < 0.815\sqrt{\frac{E}{F_u}} = 18.07 \qquad \text{Therefore E2.2.2.1} - 2 \text{ applies}$$

$$\phi P_n = \phi 2.20 t d_a F_u; \quad \boldsymbol{\phi = 0.80}$$

$$\phi P_n = (\boldsymbol{0.80})2.20(0.003")(0.465")(60 \text{ ksi})$$

$$\underline{\boldsymbol{\phi P_n = 0.147 \text{ kips}}}$$

b. E2.2.2.1-3

For $0.815 \sqrt{(E/F_u)} \leq d_a/t \leq 1.397\sqrt{(E/F_u)}$: $P_n = 0.280\left[1 + 5.59\frac{\sqrt{E/F_u}}{d_a/t}\right] t d_a F_u$

Design Factor	Existing	Recalibrated	Proposed
ϕ (LRFD) ($\beta = 3.5$)	0.55	0.865	0.85

i.   Example: Existing Design Factor.

$t = 0.03"$

$d_a = 0.738"$

$E = 29{,}500 \text{ ksi}$

$F_y = 60 \text{ ksi}$

$d_a/t = 0.738"/0.03" = 24.61$

$$0.815\sqrt{\frac{E}{F_u}} = 0.815\sqrt{29{,}500 \text{ ksi}/60 \text{ ksi}} = 18.07$$

$$1.397\sqrt{\frac{E}{F_u}} = 1.397\sqrt{29{,}500 \text{ ksi}/60 \text{ ksi}} = 30.98$$

$$0.815\sqrt{\frac{E}{F_u}} = 18.07 < d_a/t = 24.61 < 1.397\sqrt{\frac{E}{F_u}} = 30.98$$

Therefore $E2.2.2.1-3$ applies

$$\phi P_n = \phi 0.280\left[1 + 5.59\frac{\sqrt{E/F_u}}{d_a/t}\right]t d_a F_u; \ \phi = 0.55$$

$$= (0.55)0.280\left[1 + 5.59\frac{\sqrt{29{,}500 \text{ ksi}/60 \text{ ksi}}}{0.743"/0.03"}\right](0.03")(0.743")(60 \text{ ksi})$$

$\underline{\phi P_n = 1.237 \text{ kips}}$

ii.   Example: Recalibrated Design Factor.

$d_a/t = 0.738"/0.03" = 24.61$

$$0.815 \sqrt{\frac{E}{F_u}} = 0.815 \sqrt{\frac{29{,}500 \text{ ksi}}{60 \text{ ksi}}} = 18.07$$

$$1.397 \sqrt{\frac{E}{F_u}} = 1.397 \sqrt{\frac{29{,}500 \text{ ksi}}{60 \text{ ksi}}} = 30.98$$

$$0.815 \sqrt{\frac{E}{F_u}} = 18.07 < {}^{d_a}\!/_t = 24.61 < 1.397 \sqrt{\frac{E}{F_u}} = 30.98$$

Therefore E2.2.2.1 − 3 applies

$$\phi P_n = \phi 0.280 \left[1 + 5.59 \frac{\sqrt{E/F_u}}{d_a/_t} \right] t d_a F_u ; \; \phi = \mathbf{0.85}$$

$$= (\mathbf{0.85})0.280 \left[1 + 5.59 \frac{\sqrt{29{,}500 \text{ ksi}/60\text{ksi}}}{0.743"/_{0.03"}} \right] (0.03")(0.743")(60 \text{ ksi})$$

$$\underline{\mathbf{\phi P_n = 1.912 \text{ kips}}}$$

c. E2.2.2.1-4

For $d_a/t \geq 1.397 \sqrt{(E/F_u)}$: $P_n = 1.40 d_a F_u$

Design Factor	Existing	Recalibrated
ϕ (LRFD) ($\beta = 3.5$)	0.50	0.467

i.   Example: Existing Design Factor.

$t = 0.03"$

$d_a = 0.998"$

E = 29,500 ksi

F_y = 60 ksi

d_a/t = $0.998"/0.03"$ = 33.36

$1.397\sqrt{\dfrac{E}{F_u}} = 1.397\sqrt{29,500\ ksi/60\ ksi} = 30.98$

$1.397\sqrt{\dfrac{E}{F_u}} = 30.98 < d_a/t = 33.36$

Therefore E2.2.2.1 − 4 applies

$\phi P_n = \phi 1.40 t d_a F_u;\ \ \phi = 0.50$

$\phi P_n = (0.50)1.40(0.03")(0.998")(60\ ksi)$

$\underline{\phi P_n = 1.258\ kips}$

ii.   Example: Recalibrated Design Factor.

d_a/t = $0.998"/0.03"$ = 33.36

$1.397\sqrt{\dfrac{E}{F_u}} = 1.397\sqrt{29,500\ ksi/60\ ksi} = 30.98$

$1.397\sqrt{\dfrac{E}{F_u}} = 30.98 < d_a/t = 33.36$

Therefore E2.2.2.1 − 4 applies

$\phi P_n = \phi 1.40 t d_a F_u;\ \ \boldsymbol{\phi = 0.467}$

$\phi P_n = (\boldsymbol{0.467})1.40(0.03")(0.998")(60\ ksi)$

$\underline{\boldsymbol{\phi P_n = 1.174\ kips}}$

3. TENSION: FAILURE THROUGH THE WELD

a. E2.2.3-1

$$P_n = \frac{\pi d_e^2}{4} F_{xx} \text{ Where: } d_e = 0.7d - 1.5t \text{ , with } d_{eMax} = 0.55d$$

Proposed Modification: $P_n = (r)\frac{\pi d_e^2}{4} F_{xx}$ **where r =0.50**

and d_e = the greater of $\begin{vmatrix} 0.7d - 1.5t \\ \\ 0.45d \end{vmatrix}$

Design Factor (panel and deck)	Existing	Recalibrated with S100-12 de equation	Recalibrated with modified d_e equation and r =0.50.	Proposed with modified d_e equation and r =0.50
ϕ (LRFD, β = 3.0)	0.50	0.028	0.499	0.50

i. Example: Existing d_e equation and design factor with t < 0.07".

t = 0.03"

d = 0.625"

E = 29,500 ksi

F_{xx} = 60 ksi

$d_e = 0.7d - 1.5t = 0.7(0.625") - 1.5(0.03") = 0.3925"$

d_e max $= 0.55(d) = 0.55(0.625") = 0.344"$ (max controls)

$\phi P_n = \phi \frac{\pi d_e^2}{4} F_{xx}, \phi = 0.50$

$\phi P_n = (0.50)\frac{\pi(0.344")^2}{4}(60 \text{ ksi})$

$\underline{\phi P_n = 2.788 \text{ kips}^*}$

> NOTE: Equation E2.2.3-1 yields a coefficient of variation for tested strength of predicted strength equal to 1.43 and is not dependable. This explained by inaccurate effective weld diameter calculations and concentrated stresses at the weld perimeter which AISI does not currently consider in equation E2.2.3-1.

ii.   Example: Proposed d_e equation, reduction factor r = 0.50 and recalibrated design
       factor with t < 0.07".

  t = 0.03"

  Use $d_e = 0.7d - 1.5t$, with **$0.45d < d_e$**

  $d_e = 0.7d - 1.5t = 0.7(0.625") - 1.5(0.03") = 0.3925"$ (largest controls)

  d_e min $= 0.45(d) = 0.45(0.625") = 0.281"$

  $\phi P_n = \phi\ (r) \frac{\pi d_e^2}{4} F_{xx}, \phi = \mathbf{0.50, r = 0.50}$

  $\phi P_n = (0.50)\mathbf{(0.50)} \frac{\pi(0.3925")^2}{4} (60\ ksi)$ | NOTE: This a <u>more accurate</u> representation of the tension strength of the weld as "r" considers concentrated perimeter stresses.

  $\underline{\mathbf{\phi P_n = \ 1.815\ kips}}$

iii.   Example: Existing d_e equation and design factor with t > 0.07".

  t = 0.12"

  d = 0.625"

  E = 29,500 ksi

  F_{xx} = 60 ksi

  $d_e = 0.7d - 1.5t = 0.7(0.625") - 1.5(0.12") = 0.258"$ (controls)

  d_e max $= 0.55(d) = 0.55(0.625") = 0.344"$

  $\phi P_n = \phi\ \frac{\pi d_e^2}{4} F_{xx}, \phi = 0.50$

  $\phi P_n = (0.50) \frac{\pi(0.258")^2}{4} (60 ksi)$

  $\underline{\phi P_n = 1.562\ kips^*}$

NOTE: Equation E2.2.3-1 yields a coefficient of variation for tested strength of predicted strength equal to 1.43 and <u>is not dependable</u>. This explained by inaccurate effective weld diameter calculations and concentrated stresses at the weld perimeter which AISI does not consider in equation E2.2.3-1.

iv.   Example: Proposed d_e equation and recalibrated design factor with $t > 0.07$".

$t = 0.12$"

Use $d_e = 0.7d - 1.5t$, with $\mathbf{0.45d} < d_e$

$d_e = 0.7d - 1.5t = 0.7(0.625") - 1.5(0.12") = 0.258"$

$\mathbf{d_e\ min = 0.45(d) = 0.45(0.625") = 0.281"}$ **(largest controls)**

$\phi P_n = \phi\,(r)\dfrac{\pi d_e^2}{4} F_{xx}, \phi = \mathbf{0.50}, r = \mathbf{0.50}$

$\phi P_n = (0.50)(\mathbf{0.50})\dfrac{\pi(0.281")^2}{4}(60\text{ ksi})$

$\underline{\mathbf{\phi P_n = \ 0.932\ kips}}$

NOTE: This a <u>more accurate</u> representation of the tension strength of the weld as "r" considers concentrated perimeter stresses.

4. TENSION: FAILURE THROUGH THE SHEET

a. E2.2.3-2

$P_n = 0.8(F_u/F_y)^2 t d_a F_u$

Design Factor (Panel and Deck)	Existing	Recalibrated	Proposed
ϕ (LRFD, $\beta = 3.0$)	0.60	0.767	0.75

i.   Example: Existing Design Factor with Interior Sheet Configuration.

$t = 0.03"$

$d_a = 0.625"$

$E = 29,500$ ksi

$F_u = 60$ ksi

$F_y = 50$ ksi

$\phi P_n = \phi 0.8(F_u/F_y)^2 t d_a F_u ;\ \ \phi = 0.60$

$\phi P_n = (0.60)0.8\left(\dfrac{60\ ksi}{50\ ksi}\right)^2 (0.03")(0.625")(60\text{ ksi})$

$\underline{\phi P_n = 0.778 \text{ kips}}$

ii.   Example: Recalibrated Design Factor with Interior Sheet Configuration.

$t = 0.03"$

$d_a = 0.625"$

$E = 29{,}500 \text{ ksi}$

$F_u = 60 \text{ ksi}$

$F_y = 50 \ ksi$

$\phi P_n = \phi 0.8 (F_u/F_y)^2 t d_a F_u \ ; \ \ \boldsymbol{\phi = 0.75}$

$\phi P_n = (\boldsymbol{0.75})0.8 \left(\dfrac{60 \ ksi}{50 \text{ ksi}}\right)^2 (0.03")(0.625")(60 \text{ ksi})$

$\underline{\boldsymbol{\phi P_n = 0.971 \text{ kips}}}$

5. SUMMARY

Table C.1: Summary of Shear Example Calculations

	Shear Strength, ϕP_n (kips)				
	E2.2.2.1-1		E2.2.2.1-2	E2.2.2.1-3	E2.2.2.1-4
	t < 0.07"	t > 0.07"			
Existing:	2.509	1.412	0.129	1.237	1.258
Proposed:	3.27	1.675	0.147	1.912	1.174
Percent Change	**+30.3%**	**+19.0%**	**+13.9%**	**+54.5%**	**-6.7%**

Table C.2: Summary of Tension Example Calculations
Note: * = E2.2.3-1's current use of $\phi = 0.50$ does not reflect the expanded data base.

	Tension Strength, ϕP_n (kips)		
	E2.2.3-1		E2.2.3-2
	t < 0.07"	t > 0.07"	
Existing:	2.788*	1.562*	0.778
Proposed:	1.815	0.932	0.971
Percent Change	**N/A**	**N/A**	**+24.8%**

American Iron and Steel Institute

25 Massachusetts Avenue, NW
Suite 800
Washington, DC 20001

www.steel.org

The New Steel